

1. Report No. FHWA/RD-86/035	2. Government Accession No. PB 86 139 664/AS	3. Recipient's Catalog No.	
4. Title and Subtitle Safety and Operational Considerations For Design of Rural Highway Curves		5. Report Date December 1985	
		6. Performing Organization Code	
7. Author(s) John C. Glennon, Timothy R. Neuman & Jack E. Leisch		8. Performing Organization Report No.	
9. Performing Organization Name and Address Jack E. Leisch & Associates 1603 Orrington, Suite 1290 Evanston, Illinois 60201		10. Work Unit No. (TRAIS) 31J1-172	
		11. Contract or Grant No. DOT-FH-11-9575	
12. Sponsoring Agency Name and Address Federal Highway Administration Safety Design Division, HSR-20 6300 Georgetown Pike McLean, Virginia 22101		13. Type of Report and Period Covered Final Report	
		14. Sponsoring Agency Code T-0651	
15. Supplementary Notes FHWA Contract Manager: George B. Pilkington, II (HSR-20)			
16. Abstract This research was performed to study the safety and operational characteristics of two-lane rural highway curves. A series of interdependent research methodologies was employed, including (1) multivariate accident analyses; (2) simulation of vehicle/driver operations using HVOSM; (3) field studies of vehicle behavior on highway curves; and (4) analytical studies of specific problems involving highway curve operations. Among the study findings are recommendations regarding design of the highway curves. The research indicated important trade-offs among curve radius, curve length and superelevation. The value of spiral transitions was demonstrated by the studies of driver behavior. Significant path overshoot was observed at all sites regardless of the curve radius; this behavior was also modeled by HVOSM. Studies of accidents on highway curves showed single-vehicle run-off-road accidents to be of paramount concern. Roadside treatment countermeasures were found to offer the greatest potential for mitigating the frequency and severity of accidents on rural highway curves. NOTE: This publication does not contain the Appendices which are not necessary to understanding this research or implementing the results. However, the entire report, including the Appendices, may be purchased from NTIS. <i>This note not applicable</i>			
17. Key Words Design Criteria Highway Design Simulation Highway Curves Safety		18. Distribution Statement No restrictions. This document is available to the public through the National Technical Information Service, Springfield, Virginia 22161	
19. Security Classif. (of this report) Unclassified	20. Security Classif. (of this page) Unclassified	21. No. of Pages 339 261	22. Price

Acknowledgments

The successful completion of this research was the result of the effort of many individuals and organizations. The authors wish to acknowledge the assistance of all those who participated, but in particular, the following individuals whose contributions were essential to the project:

James B. Saag, Jack E. Leisch & Associates
Ray McHenry, McHenry Consultants, Inc.
Brian McHenry, McHenry Consultants, Inc.
Karin Bauer, Midwest Research Institute
Jim Heminger, Federal Highway Administration

Collection and analysis of geometric and accident data were made possible through the efforts of the following individuals and State agencies.

Robert A. Lavette, Florida Department of Transportation
John Blair, Illinois Department of Transportation
Charles Groves, Ohio Department of Transportation
Ben Barton, Texas State Department of Highways and
Public Transportation

V. COMPUTER SIMULATION STUDIES

This task of the research used the Highway-Vehicle-Object Simulation Model (HVOSM) to study various aspects of vehicle operations and control on highway curves. The objectives of this task were to:

- (1) Demonstrate the applicability of HVOSM as a tool for studying the dynamic responses of vehicles traversing highway curves;
- (2) Study the sensitivity of tire friction demand, vehicle placement, and vehicle path for critical vehicle traversals to various highway curve design parameters;
- (3) Study the sensitivity of tire friction demand and driver discomfort for moderate encroachments onto the shoulder of highway curves with various cross-slope breaks;
- (4) Study the rollover potential of moderate vehicular encroachments onto various roadside slopes on highway curves.

HVOSM Methodology

The HVOSM is a computerized mathematical model originally developed and refined by Calspan Corporation, formerly Cornell Aeronautical Laboratories (30). The HVOSM is capable of simulating the dynamic responses of a vehicle traversing a three-dimensional terrain configuration. The vehicle is composed of four rigid masses; viz., sprung mass, unsprung masses of the left and right independent suspensions of the front wheels, and an unsprung mass representing a solid rear-axle assembly.

This study used the Roadside Design version of HVOSM that is currently available from FHWA. A 1971 Dodge Coronet was used as the test vehicle throughout the study. Certain modifications were necessary to perform the range of studies undertaken in this research. These modifications are described in Appendix D and in a separate report, HVOSM Studies of Cross-Slope Breaks on Highway Curves, (31) which gives the details of the HVOSM studies of cross-slope breaks.

These modifications included the following:

- (1) Driver discomfort factor output;
- (2) Friction demand output;
- (3) Terrain table generator;
- (4) Driver model inputs (damping, steer velocity, steer initialization);
- (5) Wagon-tongue path following algorithm;
- (6) Ground contact point interpolation; and
- (7) Effective Range Angled Boundary Option (ERABO).

For the highway curve traversal studies, one of the more important aspects of the path following algorithm is the length of the wagon-tongue or probe length. The wagon-tongue is attached to the center of gravity and extends in front of the vehicle parallel to its x-axis. A probe at the end of the wagon-tongue monitors the error from the intended path and activates the driver model inputs. The probe length in essence simulates the complex interaction which occurs as a driver sees the roadway ahead and responds to what he sees. Selection of a probe length, therefore, actually amounts to a decision as to what type of driver is being modeled. Long probe lengths are indicative of "ideal" drivers, who prepare for the curve well in advance. The resulting simulated behavior closely follows that described by the centripetal force equation, with the simulated vehicle path tracking nearly exactly the center of the lane. Moderate probe lengths create minor path corrections just preceding the curve, and tend to allow the vehicle to track in a near optimum manner. Calculated friction values are somewhat higher than is predicted by the centripetal force equation. Very short probe lengths represent aggressive or inattentive driver behavior. Path corrections in response to the presence of the impending curve occur only as the vehicle actually enters the curve. The result is a dynamic over-shoot at the beginning of the curve, with high lateral friction demand generated by the vehicle and a distinctly noncircular path.

The above discussion emphasizes the need to carefully define the driver behavior being modeled. Highly variable results can be obtained running different probe lengths on the same simulated curve at the same speed.

Preliminary Curve Runs and Results

Twelve initial HVOSM runs were made to demonstrate and verify that the HVOSM yields reasonable dynamic responses for curve traversals. These runs were made on unspiraled highway curves with AASHTO (32) superelevation runoff lengths distributed 70 percent on tangent and 30 percent on curve. The basic idea was to select a long probe length that would allow the vehicle to track the center of the lane with very little path deviation. The resulting vehicle dynamics given by the HVOSM could then be compared to those predicted by the centripetal force equation.

Table 22 shows the calculated and simulated dynamic responses for running the vehicle at design speed for the twelve test curves using a probe that represented a 1.0 second driver preview. As can be seen, the calculated lateral acceleration, $V^2/15R$ ($V^2/127R$) and the simulated lateral acceleration are closely comparable for all tests. Also, the calculated tire responses, $(V^2/15R)-e$ [$(V^2/127R)-e$] are comparable to the simulated tire responses.

It is noteworthy that, because of roll angle, the driver discomfort factor (centrifugal acceleration acting on the driver) is always higher than the lateral acceleration on the tires. Therefore, the design f values in the AASHTO process are not the centrifugal acceleration where the driver begins to feel discomfort, but represent the lateral friction on the tires that creates the threshold of driver discomfort.

Critical Curve Runs and Results

With the HVOSM verified for use on curve traversals, the model appeared to be a reasonable tool for studying curve traversals where the vehicle does not precisely follow the center of the lane. The purpose of this exercise was to use the HVOSM to study the sensitivity of vehicle dynamics to varying curve and operational parameters.

It was first necessary to define a nominally critical level of driver behavior. Behavior less critical, or near average, would result in simulations which tend to mirror dynamics predicted by the centripetal force equation. Highly critical

TABLE 22

INITIAL HVOSM TESTS

	V Speed		R Roadway Radius ft (m)	e Superelevation percent	Calculated Results*		HVOSM Results		
	mph	(km/h)			Lateral Acceleration	Tire Friction	Maximum Lateral Acceleration	Maximum Tire Friction	Maximum Driver Discomfort Factor
82	20	(33)	108 (33)	8	0.25	0.17	0.25	0.17	0.20
	20	(33)	128 (39)	4	0.21	0.17	0.20	0.14	0.18
	31	(50)	230 (70)	10	0.26	0.16	0.26	0.17	0.20
	31	(50)	272 (83)	6	0.22	0.16	0.22	0.17	0.20
	42	(67)	469 (143)	8	0.23	0.15	0.23	0.16	0.18
	42	(67)	574 (175)	4	0.19	0.15	0.19	0.16	0.19
	52	(83)	650 (198)	10	0.26	0.16	0.27	0.17	0.21
	52	(83)	850 (259)	6	0.20	0.14	0.20	0.14	0.18
	62	(100)	1207 (368)	8	0.20	0.12	0.22	0.10	0.15
	62	(100)	1529 (466)	4	0.16	0.12	0.18	0.12	0.16
	73	(117)	1637 (499)	10	0.20	0.10	0.20	0.11	0.12
	73	(117)	2083 (635)	6	0.16	0.10	0.16	0.11	0.13

* Calculated results are based on centripetal force equation

1 mph = 1.609 km/h

1 ft = 0.305 m

levels, on the other hand, may not produce realistic results, and thus may not provide a useful basis for comparing variable geometrics.

The selection of an appropriate level of criticality was based on previous vehicle operations research. Studies by Glennon (33) in Texas indicated that most drivers exceed the AASHTO design f , and that some exceed it greatly. The report relates maximum path curvature to highway curvature for various percentiles of the driving population. For purposes of this study the 95th percentile path was selected to represent nominally critical operations. This relationship is as follows:

$$R_V = 5820 R_C / (R_C + 6780) \quad [5.1]$$

Where

R_V = 95th percentile vehicle path radius (ft)

R_C = highway curve radius (ft)

NOTE: 1 ft = 0.305 m

Using the path described by Equation 5.1, the critical f factors were calculated by substituting path curvature for highway curvature in the centripetal force equation for any design speed combination of highway curvature and super-elevation.

With this relationship between highway curve parameters and nominally critical factors established, several preliminary HVOSM runs were made to select a probe length that best generated the intended critical operations. The selected probe length represents a 0.25 second driver preview, and is expressed as follows:

$$L = 0.25V$$

Where

L = Probe Length, ft (m)

V = Forward Velocity, ft/s (m/s)

With the probe length established, the HVOSM was ready for studying the sensitivity of vehicle dynamics to various highway curve design and operational parameters under nominally critical path following conditions. Of particular interest were:

- (1) Vehicle speed
- (2) Superelevation runoff length
- (3) Superelevation runoff distribution
- (4) Presence of spirals
- (5) Length of spirals
- (6) Presence of downgrade
- (7) Length of curve

Twenty-four HVOSM runs were made using six AASHTO metricated curves. The results of these runs are shown in Table 23 and discussed below. Figure 8 shows examples of the HVOSM output.

Vehicle Speed

The centripetal force equation demonstrates the sensitivity of vehicle dynamics to speed. For actual highway curve operations, it is reasonable to expect a portion of drivers to exceed the nominal design speed of the curve. (Of course, the frequency and amount of "excessive" speed behavior varies with the type of

TABLE 23

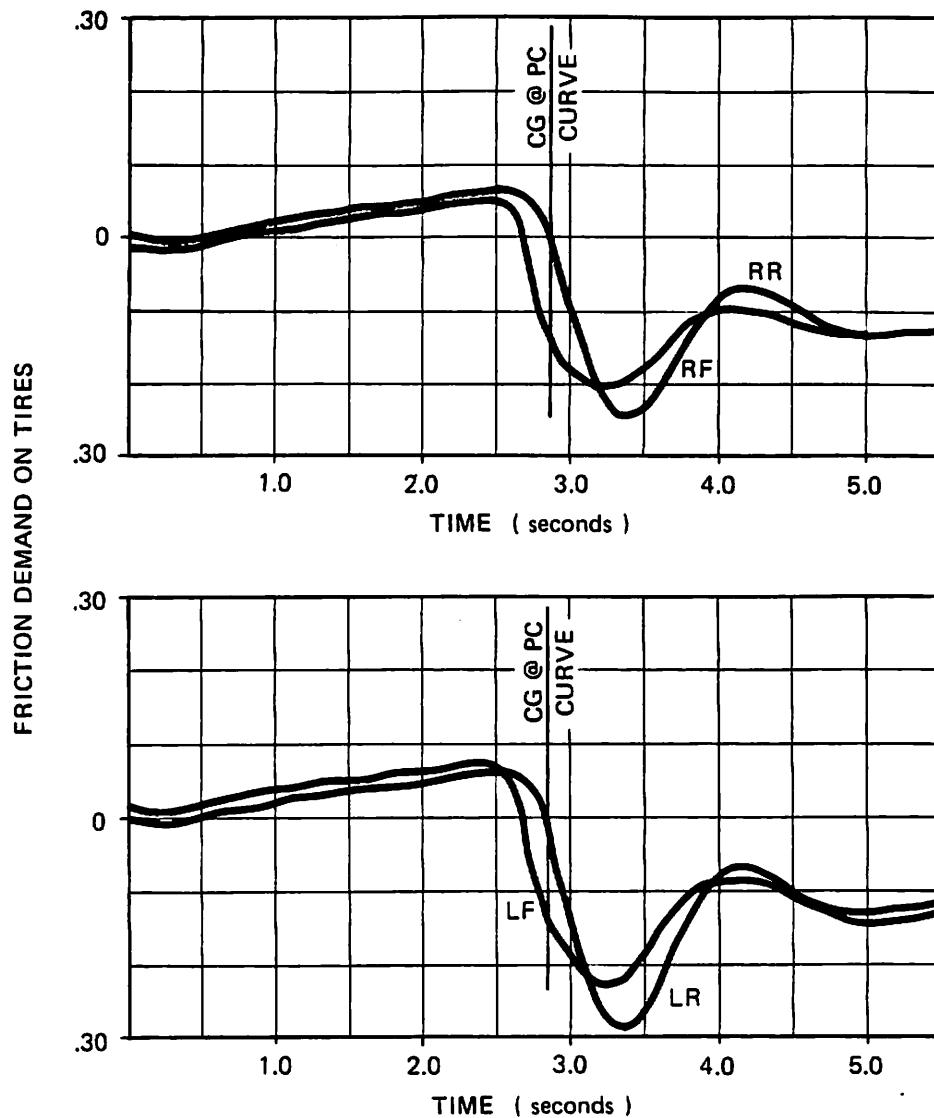
CRITICAL HVOSM TESTS

	TEST PARAMETERS							RESULTS		
	Curve Radius	Maximum Super-elevation (Percent)	Curve Design Speed	Length of Super-elevation Runoff	Percent of Maximum Super-elevation on Tangent	Presence and Length of Spiral	Grade (Percent)	Test Vehicle Operating Speed	AASHTO Design f	HVOSM f
	ft (m)		mph(km/h)	ft (m)				mph(km/h)		
85	2461 (750)	6	75 (120)	200 (61)	70	None	0	87 (140)	0.092	0.190
	2461 (750)	6	75 (120)	200 (61)	70	None	0	75 (120)	0.092	0.150
	1968 (600)	10	75 (120)	302 (92)	70	None	0	87 (140)	0.092	0.230
	1968 (600)	10	75 (120)	302 (92)	70	None	0	75 (120)	0.092	0.160
	1968 (600)	10	75 (120)	302 (92)	20	None	0	75 (120)	0.092	0.190
	1968 (600)	10	75 (120)	164 (50)	70	None	0	75 (120)	0.092	0.120
	1345 (410)	8	62 (100)	216 (66)	70	None	0	75 (120)	0.116	0.260
	1345 (410)	8	62 (100)	216 (66)	70	None	0	62 (100)	0.116	0.170
	1345 (410)	8	62 (100)	108 (33)	70	None	0	62 (100)	0.116	0.140
	1345 (410)	8	62 (100)	216 (66)	N/A	AASHTO	0	62 (100)	0.116	0.100
	689 (210)	10	50 (80)	236 (72)	70	None	0	62 (100)	0.140	0.390
	689 (210)	10	50 (80)	236 (72)	70	None	0	50 (80)	0.140	0.240
	689 (210)	10	50 (80)	236 (72)	20	None	0	50 (80)	0.140	0.260
	689 (210)	10	50 (80)	236 (72)	70	None	5	50 (80)	0.140	0.240
	689 (210)	10	50 (80)	236 (72)	N/A	AASHTO	0	50 (80)	0.140	0.120
	689 (210)*	10	50 (80)	236 (72)	70	None	0	50 (80)	0.140	0.200
	689 (210)	10	50 (80)	236 (72)	20	None	5	62 (100)	0.140	0.430
	426 (130)	8	37 (60)	164 (50)	70	None	0	50 (80)	0.152	0.400
	426 (130)	8	37 (60)	164 (50)	70	None	0	37 (60)	0.152	0.200
	426 (130)	8	37 (60)	164 (50)	70	None	5	37 (60)	0.152	0.210
	426 (130)	8	37 (60)	164 (50)	N/A	AASHTO	0	37 (60)	0.152	0.120
	164 (50)	10	25 (40)	164 (50)	70	None	0	37 (60)	0.164	0.520
	164 (50)	10	25 (40)	164 (50)	70	None	0	25 (40)	0.164	0.200
	164 (50)	10	25 (40)	164 (50)	70	None	5	25 (40)	0.164	0.200

* 164 ft (50 m) curve length

1 ft = 0.305 m

1 mph = 1.609 km/h



TEST CONDITIONS

Speed - - 50mph (80km/h)

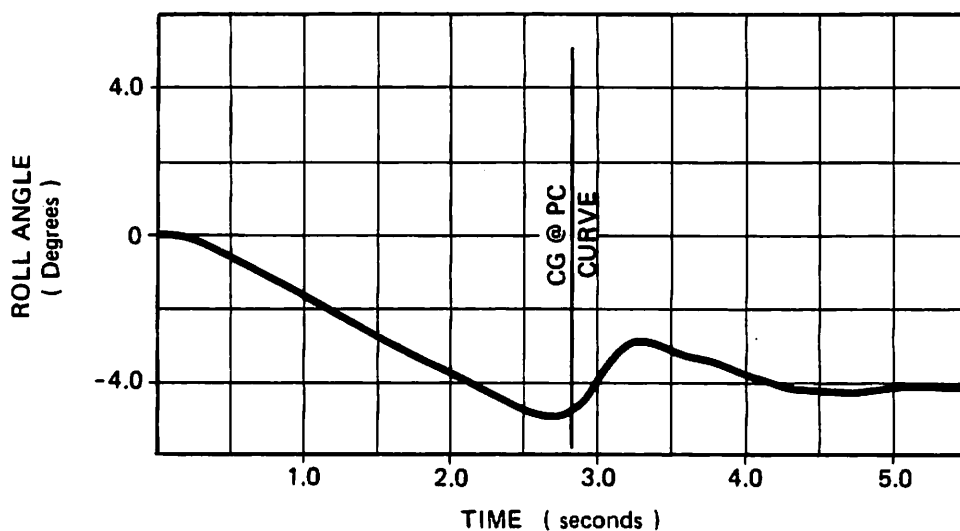
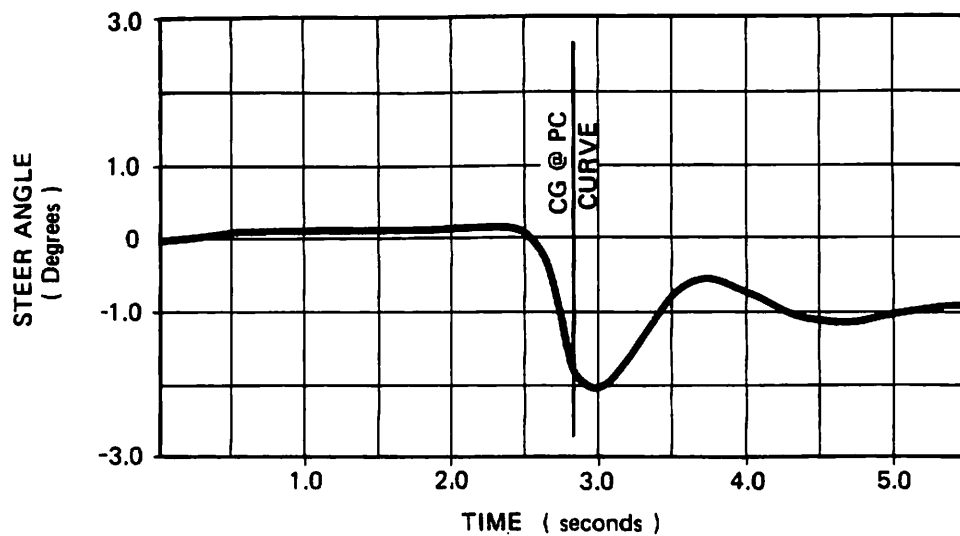
Roadway Geometry

Centerline Radius 689ft (210m)
 Superelevation 10 percent
 Super. Runoff 236ft (72m)
 Super. Dist. 70% on tangent
 Grade 0 percent

Vehicle and Driver Characteristics

Probe Length 17.7ft (5.4m)
 P GAIN 5.8×10^{-6} rad / ft
 (1.9×10^{-5} rad / m)
 Q GAIN 5.8×10^{-7} rad · s / ft
 (1.9×10^{-6} rad · s / m)
 No Deceleration

Figure 8. EXAMPLE HVOSM OUTPUT



TEST CONDITIONS

Speed - - 50mph (80km/h)

Roadway Geometry

Centerline Radius 689ft (210m)
 Superelevation 10 percent
 Super. Runoff 236ft (72m)
 Super. Dist. 70% on tangent
 Grade 0 percent

Vehicle and Driver Characteristics

Probe Length 17.7ft (5.4m)
 P GAIN 5.8×10^{-6} rad / ft
 (1.9×10^{-5} rad / m)
 Q GAIN 5.8×10^{-7} rad · s / ft
 (1.9×10^{-6} rad · s / m)
 No Deceleration

Figure 8. EXAMPLE HVOSM OUTPUT (Continued)

highway, the curve itself, and environmental conditions.) Simulations of dynamic responses to speeds in excess of design were therefore believed valuable.

To test high-speed vehicle behavior, each of the six test highway curves was run at 12.5 mph (20 km/h) above design speed. This speed increment is slightly greater than is considered the "potential increase permissible within design speed" by Leisch (34), and thus represents an upper limit on reasonable speed expectations for almost all highway curves.

The tire friction for this speed increment was found to be most sensitive for the lower design speed curves. For the 25 mph (40 km/h) design speed curve, the friction demand was simulated to be 0.52 compared with a design f of 0.16. These results could also be similarly predicted with the centripetal force equation (thus providing one more verification of the HVOSM methodology.)

The implications of the test results for speed are very important. These suggest that an existing highway curve that is underdesigned for the prevailing operating speed could present a severe roadway hazard. This is particularly true for design speeds below 60 mph (about 100 km/h). At such lower design speeds, frequent vehicle operating speeds of 5 to 10 mph (8 to 16 km/h) above the curve design speed can be reasonably expected.

Superelevation Runoff Length

This parameter was evaluated for design speeds of about 50 mph (80 km/h) and 60 mph (100 km/h) by comparing the AASHTO runoff length with one that was half as long. For the comparison, the superelevation runoff length was distributed with 70 percent on the tangent and 30 percent on the curve.

The somewhat surprising result of these tests was that the shorter runoff length yielded slightly smaller friction demands. The only identifiable explanation for this phenomenon is that the maximum simulated friction demands take place in the initial part of the curve where the shorter runoff length provided slightly higher superelevation.

Superelevation Runoff Distribution

This parameter was evaluated for 50 mph (80 km/h) and 75 mph (120 km/h) highway curves having AASHTO superelevation runoff lengths with 70-30 and 20-80 distributions. As expected, 70-30 distribution, where most of the superelevation transition is provided on the tangent, produced somewhat smaller friction demands. The differences can be explained almost entirely by the difference in superelevation in the initial part of the curve where the maximum friction demand was generated.

Presence of Spirals

This parameter was evaluated for highway curves with design speeds between 37 mph (60 km/h) and 62 mph (100 km/h). The comparison was between highway curves with and without AASHTO spirals.

This comparison provides the most dramatic results of the study. *In all cases, the presence of the spiral reduced the friction demand from a value significantly higher than the design f to one that was below the design f .*

The reason for this dramatic result seems readily evident. For the driver who is inattentive or for some other reason has limited notice of the upcoming curve, the spiral not only reduces his absolute path error over time but requires less severe steering to correct for the desired path because the path of a spiral is less severe than the path of a circular curve.

Length of Spiral

Although the initial plan was to test a spiral that was twice the length of an AASHTO spiral, this plan was not carried through after obtaining the dramatic results for the presence of AASHTO spirals.

Presence of Downgrade

This parameter was evaluated for highway curve design speeds of 25 mph (40 km/h) to 50 mph (80 km/h). In comparing a 5 percent downgrade with level terrain, no difference was found in the friction demand.

Short Curve Length

This parameter was evaluated by looking at the difference between vehicular response to the approach to a curve (i.e., the dynamics of proceeding from tangent to curve) and the response by the driver as he transitions in and immediately out of the curve. A 164-foot (50-metre) curve length of a 50 mph (80 km/h) design curve was selected for analysis.

The results of this test indicate that the inattentive driver will generate less dynamic overshoot on the very short curve because he begins sensing and adjusting for the upcoming tangent before he has to perform the maximum correction that would be necessary on a longer curve.

Summary of Critical Curve Runs

The critical analysis of highway curves provided two preliminary results with important implications. These results were subject to the field verification of the HVOSM driver inputs discussed in Chapter VI. The first important result is that the dynamic response of vehicles traversing a highway curve is very sensitive to speed. The implication of this result is that existing highway curves that are severely underdesigned for the prevailing highway speeds present serious hazards. The second important result is that the addition of spiral transitions to highway curves dramatically reduces the friction demand of critical vehicle traversals.

Cross-Slope Break Studies

Details of cross-slope break studies are reported in a separate report titled "HVOSM Studies of Cross-Slope Breaks on Highway Curves" (31). These studies and their results are summarized here.

The objective of these studies was to evaluate AASHTO (32,35) policy regarding the maximum recommended difference of 7 percent between the cross slopes of the pavement and the shoulder. This policy has existed since 1954 and is consistent with the AASHTO minimum pavement cross slope of 1 percent for high-type surfaces and the maximum AASHTO shoulder cross slope of 8 percent specified for turf shoulders.

When designing superelevated horizontal curves according to AASHTO, the cross-slope break requirement can constrain the shoulder cross-slope design on the outside of the curve. For example, with 6 percent superelevation, the cross-slope break requirement limits the maximum negative shoulder cross slope to 1 percent, which does not meet the AASHTO drainage requirements for even paved shoulders. The alternatives are to either design a positive shoulder slope or a rounded shoulder. A positive shoulder slope drains more runoff water across the pavement and creates problems with the melting of stored snow on the outside shoulder. The rounded shoulder design is more difficult to construct and maintain.

HVOSM Test Conditions and Performance Criteria

Table 24 shows the general highway geometrics, the parameters of vehicle operations, and the performance criteria selected for testing. The vehicle operating parameters were chosen to represent the design criteria of a moderate encroachment onto the shoulder. The performance criteria were selected as reasonable dynamic response thresholds for design.

HVOSM Runs

A series of initial HVOSM runs was made using the highest design speed and an extreme (16 percent) cross-slope break to study the dynamic differences between (1) four-wheel and two-wheel traversals onto the shoulder, and (2) entry to and exit from the shoulder. The results of these runs indicated that the four-wheel traversal and the entry to the shoulder produced the more extreme dynamic responses. In the main part of the experiment, 14 runs were made using design speeds of 50 mph to 75 mph (80 km/h to 120 km/h), shoulder slopes of 2 to 6 2 to 6 percent, and superelevation rates of 2 to 10 percent.

HVOSM Results and Design Implications

The results clearly show that the driver discomfort level (centrifugal acceleration) in a moderate shoulder traversal on highway curves is sensitive to speed, radius of curve, shoulder cross slope, and the lateral extent of movement onto the shoulder. For a given path and speed of shoulder traversal, therefore, the driver discomfort mainly increases with shoulder slope and very little, if any, with the amount of cross-slope break.

TABLE 24

HVOSM TEST CONDITIONS AND PERFORMANCE CRITERIA
FOR CROSS SLOPE BREAK STUDIES

<u>Test Conditions</u>	<u>Specification</u>
Highway Curve Radius	AASHTO Controlling Curves
Superelevation	AASHTO Controlling Curves (2 percent to 10 percent)
Shoulder Width	9.0 ft (2.7 m)
Shoulder Cross Slope	-2 percent to -6 percent
Vehicle	1971 Dodge Coronet
Initial Vehicle Speed	Design Speed
Vehicle Deceleration	Engine Braking @ 0.1 g
Vehicle Path Radius	95th percentile path as a function of highway curve radius measured by Glennon and Weaver (33)
Vehicle Path Radius Tangent Point	Corrective Curve 7.2 ft (2.2 m) from edge of roadway
<u>Performance Criteria</u>	
Tire-Pavement Friction	0.4
Driver Discomfort Factor	0.3

For paved shoulders with widths of 5.2 feet (1.6 m) or greater, where the shoulder cross slope is intended to accommodate up to a four-wheel traversal onto the shoulder, the research indicates a maximum tolerable cross-slope break of 8 percent. (Note: the tolerable cross-slope break is a function of design speed, design curvature, design superelevation and the maximum tolerable shoulder slope for these conditions.) For superelevation rates between 2 and 6 percent, this criterion allows maximum (negative) shoulder slopes ranging from 6 to 2 percent, respectively. For superelevation rates exceeding 6 percent, a different kind of shoulder cross-slope design is required.

For paved shoulders less than 5.2 feet (1.6 m) wide, which are implicitly designed to only accommodate two-wheel traversals within the bounds of the shoulder, the research indicates tolerable cross-slope breaks ranging from 8 to 18 percent. These greater cross-slope breaks do not further compromise safety beyond the initial decision of choosing the narrower shoulder.

Roadside Slope Studies

The sensitivity of vehicle dynamics to negative cross slopes shown in the cross-slope break studies raised some questions about vehicle dynamics on the more severe roadside slopes. Also, previous studies (36,37) had indicated that highway curvature was the most predominant factor in fatal rollover collisions. Therefore, a few HVOSM runs were undertaken to look at the severity of vehicle dynamic responses on roadside slopes of 4:1 and 6:1.

Since this exercise was an adjunct to the main research effort, a very limited study was done. The key purpose of these runs was to generally identify whether roadside slope design and embankment guardrail warrants might need to vary as a function of highway curvature.

Four HVOSM runs were performed in an identical manner to the cross-slope break runs using a -2 percent shoulder slope in place of the superelevation and either a 6:1 (i.e., a -16.7 percent) or a 4:1 (i.e., a -25 percent) roadside slope in place of the shoulder slope. The results of these tests are shown in Table 25.

TABLE 25
HVOSM ROADSIDE SLOPE TESTS

Side Slope Ratio	Side Slope Angle (Degrees)	Curve Design Speed mph (km/h)	Curve Radius ft (m)	Path Radius ft (m)	Maximum Lateral Acceleration on Tires(g's)	Maximum Roll Angle (Degrees)
6:1	9.5	50 (80)	689 (210)	538 (164)	0.47	14.5
6:1	9.5	75 (120)	1968 (600)	1312 (400)	0.60	15.0
4:1	14.0	50 (80)	689 (210)	538 (164)	0.60	19.5
4:1	14.0	75 (120)	1968 (600)	1312 (400)	0.78	20.0

1 mph = 1.609 km/h

1 ft = 0.305 m

With a hard surface, these runs indicated a very severe lateral acceleration on the tires for even the 6:1 slope, which is considered a mild roadside slope. Therefore, for most well-stabilized roadside surfaces free of irregularities, skidding is very likely.

The test runs also showed fairly severe vehicle roll angles on the hard flat roadside surfaces. These vehicle roll tendencies in combination with tire-plowing on unstablized roadside surfaces or impact with surface irregularities would produce a high expectation of vehicle rollover.

Although these tests were simplistic in nature, they strongly indicate a need to review roadside slope design policies and highway guardrail warrants as they apply to highway curves.

VII. COMPARISON OF HVOSM AND VEHICLE TRAVERSAL STUDIES

A primary objective of the vehicle traversal studies was to provide a basis for evaluating the previously completed HVOSM simulations (Chapter V). HVOSM has already been proven an accurate, cost-effective tool for studying vehicle behavior under highly unstable (i.e., loss of control, high speed impact) situations. Using controlled, full-scale tests for calibration, HVOSM can accurately predict the dynamic responses and consequences for a range of conditions.

In such critical applications, dynamic vehicle responses are essentially a function of vehicle properties and test conditions (e.g., speed at impact, angle of impact). Application of HVOSM to the evaluation of highway curve traversals, however, involves an additional important dimension. If the simulations are to have any real meaning, driver behavior must be reasonably modeled.

Driver Model

Modeling the driver is a particularly difficult problem, as it entails consideration of human factors such as perception and reaction time, psychological attitudes, and interaction with the vehicle. The task is more difficult given that a useful simulation tool must not be overly complex, and should be reasonably valid over the range of possible test conditions.

A complete discussion of development work is given in Appendix D. Previous research on modeling the driver (31) was adjusted and tested. Elements of the driver model employed in the simulations included a "wagon-tongue" algorithm, a neuromuscular filter, and steering parameters such as damping, steer velocity, and steer initialization.

One element of the driver model was particularly important to calibrate. Earlier discussion of HVOSM in Chapter V emphasized the importance of establishing a reasonable probe length. To review, probe length is one part of the wagon-tongue control algorithm. Its function is to simulate the driver preview

of the alignment ahead. Previous research on actual driver behavior formed the basis for selection of a speed-sensitive probe length function for the initial set of simulations reported in Chapter V.

The importance of properly selecting probe length is illustrated by Figure 31, which shows results of early calibration runs for probe length, for which various length functions were tested. Variations in probe length from 0.20 V to 0.40 V produce significantly different levels of simulated lateral acceleration (expressed as maximum f developed on the rear tires). Given this sensitivity of probe length to resultant vehicle dynamics, efforts to validate the previous runs focused on validating the probe length function. Driver behavior observed in the vehicle traversal studies formed the basis for this validation.

Comparison of Results

Insights concerning driver/vehicle behavior on curves can be obtained from evaluation of both the HVOSM curve runs and the results of the vehicle traversal studies. In order to gain these insights, it is first important to understand what each type of analysis represents.

Characteristics

As Table 37 shows, the two types of analysis are not directly comparable. HVOSM was applied to a series of AASHTO controlling curves for a range of design speeds. The field studies involved a range of highway curvature with generally less than full superelevation. Variations in both speed and path were observed, and used to determine distributions of lateral acceleration or friction factor. The accuracy and meaning of the field data were limited by collection and data reduction methodology employed. Thus, transient behavior observed in the field actually represents average friction demand for the vehicle, averaged over 1.0 to 1.7 seconds of real time. This compares with the reported friction results for HVOSM, which relate more closely to actual loss of control (0.25 seconds of real time; friction demand at the critical axle).

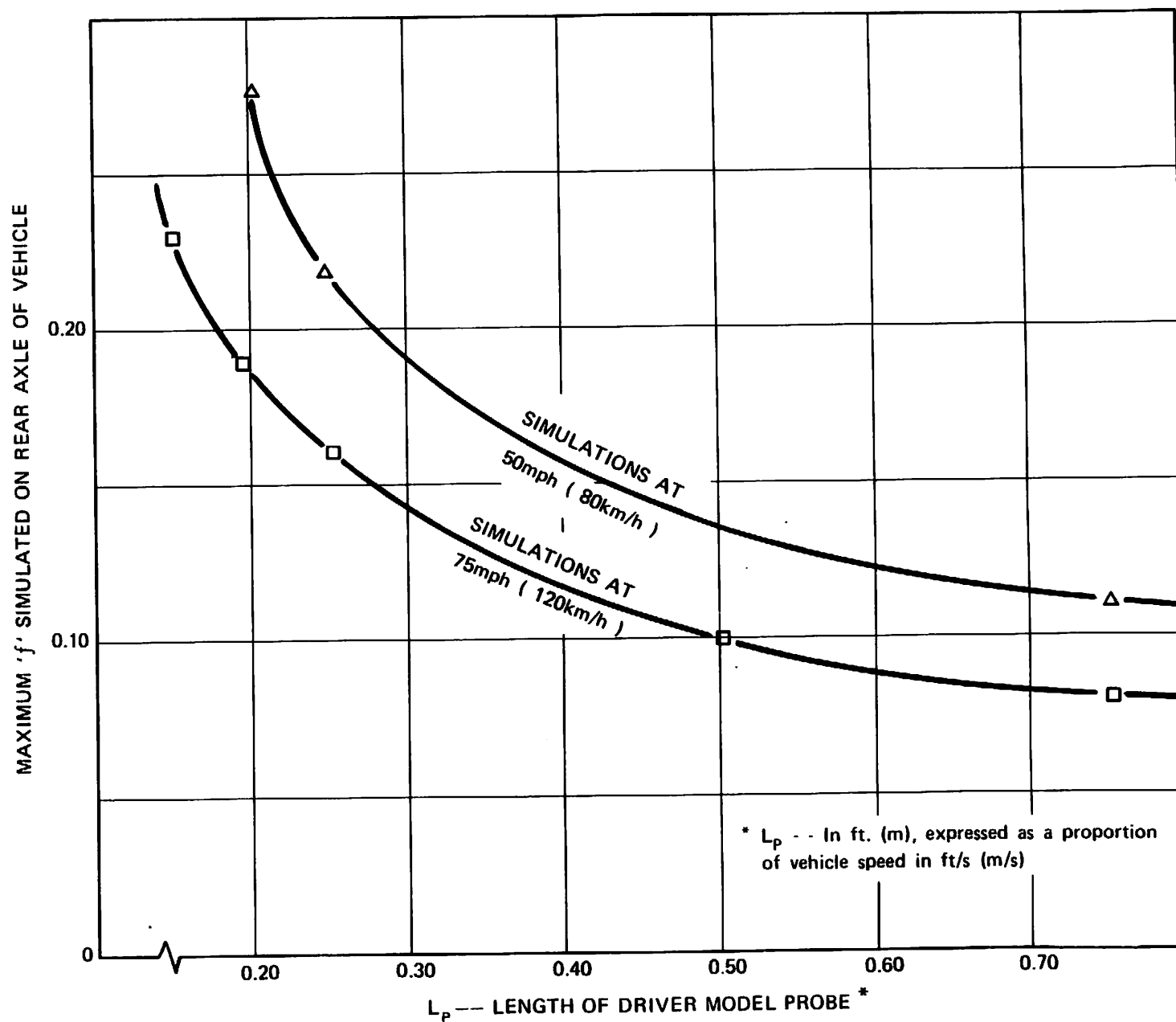


Figure 31. SENSITIVITY OF HVOSM VEHICLE DYNAMICS TO DRIVER MODEL PROBE LENGTH

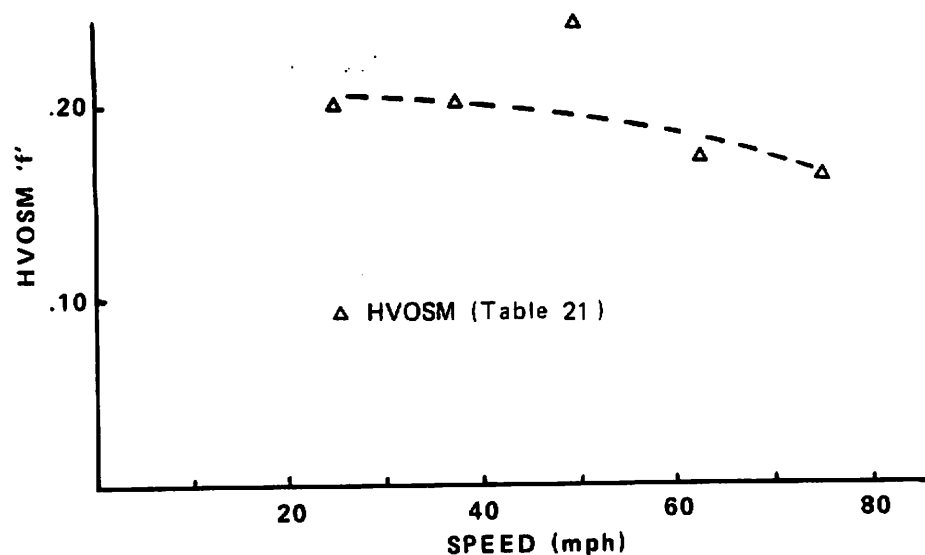
TABLE 37
CHARACTERISTICS OF HVOSM ANALYSES
AND VEHICLE TRAVERSAL STUDIES

	<u>HVOSM Curve Runs</u>	<u>Vehicle Traversal Studies</u>
Curves Analyzed	AASHTO Controlling Curves for Range of Design Speeds	Range of Curvature (No controlling curves)
Data Collected	Friction demand on 4 tires; Driver Comfort Factor; Roll and Steer Angle	Average Friction Demand (point mass)
Time Sensitivity of Data	Transient behavior observable to 0.25 seconds of real time	Measurements based on 100 ft. (30.5 m) arc--1.0 to 1.7 seconds real time
Results Reported	Maximum friction factor on 2nd highest tire of rear axle; average over 0.25 seconds	Friction factor and radius at point of maximum friction; average over 100 ft. (30.5 m) arc

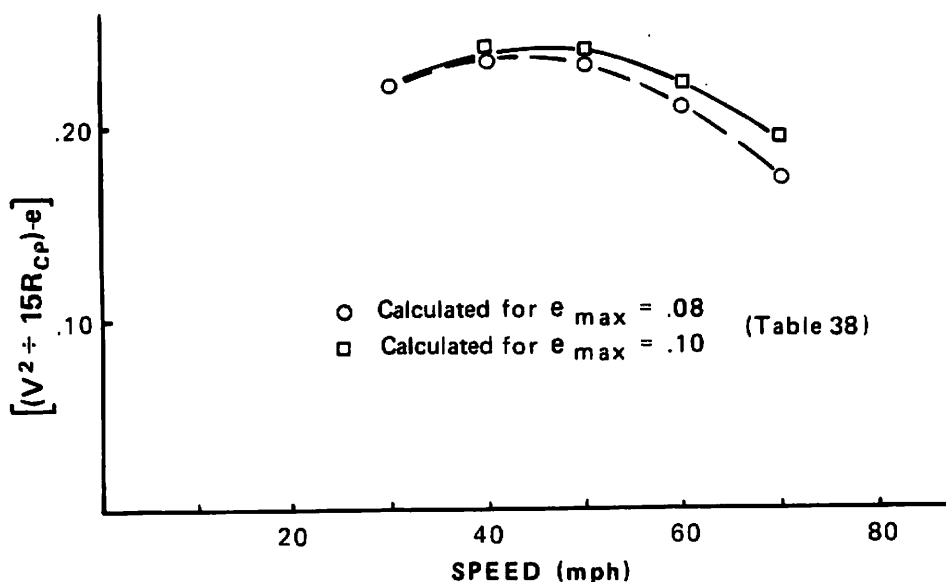
Findings

Given the differences between the analyses, direct comparisons are difficult. However, because both analyses measured transient, extreme behavior across a range of speed and curvature, it is possible to compare overall levels of friction demand, and trends across the range in speeds.

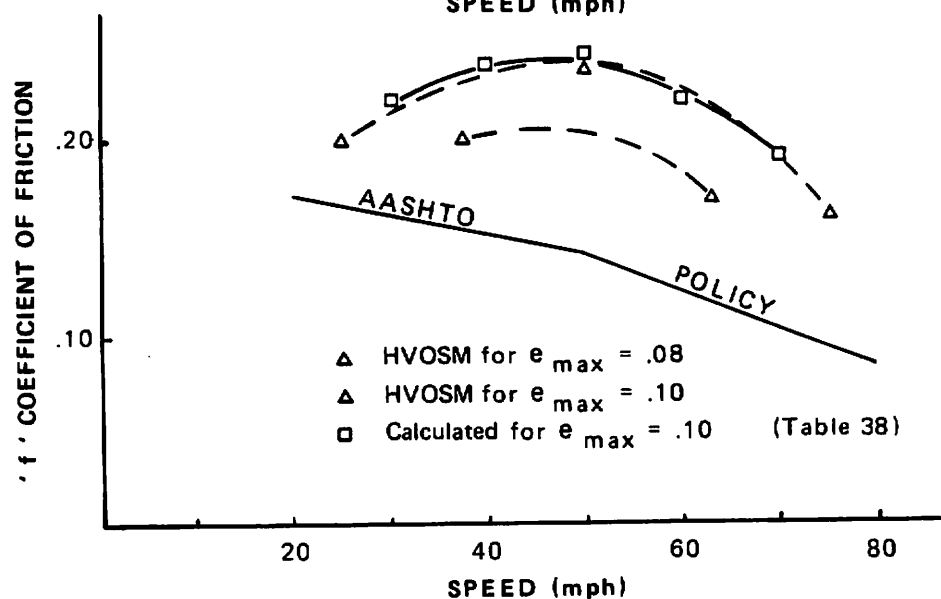
The upper portion of Figure 32 contains a plot of reported maximum friction demand vs. design speed for a sample of the HVOSM runs. The points plotted represent those simulations at which the vehicle was run at design speed on the appropriate controlling curve, with AASHTO superelevation and transition design. Initial inspection of these points shows a consistent trend for f vs. design speed, with one striking exception. Simulated f for 50 mph (80 km/h) is greater by 0.04 to 0.05 than the overall trend seems to indicate.



Maximum Friction simulated at 50mph (80km/h) does not appear consistent with the trend of 'f' vs. speed for AASHTO controlling curves.



Friction demand calculated from 95th percentile path shows different shape than hypothesized above.



Friction demand vs. speed based on above curves verifies HVOSM findings.

Note: 1mph = 1.609km/h

Figure 32. COMPARISON OF VEHICLE DYNAMICS FROM HVOSM AND VEHICLE TRAVERSAL STUDIES

Review of the vehicle traversal studies provides an explanation for the apparent anomaly. It was shown previously that vehicles tend to overshoot highway curves, producing path radii smaller than that of the curve. If this behavior is considered within the framework of AASHTO design policy, it results in an explanation for the HVOSM runs, and reveals important findings regarding design of highway curves. Consider AASHTO design controlling curves for a range of design speeds and maximum superelevation rates. If one calculates friction demand at design speed assuming overshoot driving behavior, an interesting picture of vehicle dynamics emerges. Table 38 shows such calculations, with an assumed 95th percentile driver path. As the table indicates, calculated friction demand varies for a given design speed depending on the superelevation policy (and resulting controlling curve) used. Design policies based on maximum superelevation rates (say, e_{\max} of 10 percent) result in greater calculated friction demand at design speed than policies based on lower maximum rates (say, e_{\max} of 6 percent), assuming the same overshoot driving behavior.

What Table 38 says is, assuming one is interested in nominally critical driver behavior as given by a 95th percentile driver, friction demand vs. speed relationships are not consistent for the range of superelevation policies. The middle portion of Figure 32 illustrates these side friction vs. speed relationships.

While the above discussion is relevant in itself in terms of design for curves, it is of particular value in understanding the HVOSM curve runs. As the bottom portion of Figure 32 shows, the family of points that were believed to simulate one relationship in fact represent two separate curves. The two curves describe simulated friction vs. speed for controlling curvature as defined by superelevation rate policies of 8 percent and 10 percent. Furthermore, the shape and values of the calculated curves based on the vehicle traversal studies very closely match the relationship described by the HVOSM points based on e_{\max} of 10 percent.

TABLE 38
RELATIONSHIPS AMONG SPEED, SUPERELEVATION
AND FRICTION DEMAND FOR
95TH PERCENTILE DRIVING BEHAVIOR

<u>Design Speed (mph)</u>	<u>e_{max} (percent)</u>	<u>Radius of Highway Curve(ft)</u>	<u>Radius of Vehicle Path¹(ft)</u>	<u>f at Design From Vehicle Path²</u>	<u>Speed AASHTO Criteria</u>
70	10	1637	1117	0.192	0.10
	8	1910	1295	0.172	0.10
	6	2083	1409	0.172	0.10
60	10	1091	755	0.218	0.12
	8	1206	831	0.209	0.12
	6	1348	924	0.200	0.12
50	10	694	493	0.238	0.14
	8	758	535	0.232	0.14
	6	833	584	0.225	0.14
40	10	427	317	0.237	0.15
	8	464	341	0.233	0.15
	6	508	370	0.228	0.15

¹ $R_{path} = 35 + 0.66 R_{curve}$ (From Table 36)

² Calculated friction demand assuming nominally critical path behavior at design speed. In other words,
 $f_{path} = [V^2_{design} / (15 R_{path})] - e_{max}$

1 mph = 1.609 km/h

1 ft = 0.305 m

One additional finding of both analyses is the relationship between speed and friction demand, given nominally critical driving behavior. Present design policy calls for decreasing design friction factor with increasing speed. As the lower portion of Figure 32 shows, however, friction demand does not decrease with speed, but rather peaks in the range of 45 to 55 mph (72 to 89 km/h), before decreasing for higher speeds.

Verification of Probe Length Function.--Figure 32 and the above discussion demonstrate the validity of HVOSM in simulating nominally critical vehicle dynamics expressed in terms of maximum friction demand on highway curves. Furthermore, the probe length function used in the simulations is shown to be sensitive and accurate across the range of speeds that were simulated.

Path Radius Simulation.--Simulation of nominally critical f levels was achieved with reasonable correlation to the field studies. Questions were raised, however, as to whether the simulated friction demand was a function of path overshoot similar to that observed in the field, or whether some hidden dynamic response was being simulated. These questions were answered by analyzing sample outputs from two of the runs. Among the data produced by HVOSM are X, Y coordinates for the tires and center of gravity. A simple algorithm was developed to calculate vehicle path coordinates for these data sets. The results of minimum calculated vehicle path radius from the HVOSM output are almost identical to predicted 95th percentile path radius as given by the vehicle traversal study results (see Table 36).

Nominally Critical Path Radius			
Radius of Highway Curve		Speed	
ft	(m)	mph	(km/h)
		Simulated (HVOSM)	
ft	(m)	ft	(m)
		Calculated Field Studies	
ft	(m)	ft	(m)
689	(210)	49.7	(80)
		481	(147)
		490	(149)

Vehicle Transitioning.--While HVOSM successfully simulates critical levels of f , and does so through nominally critical path radii, it does not exactly replicate the manner in which the f and critical radius are generated. Figure 33 shows plots for two vehicles--one observed in the field, and one simulated. Each vehicle's instantaneous curvature is plotted at various locations along the transition and into the curve. Simulated vehicle behavior, represented by vehicle 'A', shows almost all vehicle curvature developed after the PC, but with extremely rapid, severe spiraling. Vehicle 'B' is the vehicle which most closely represents 95th percentile path behavior at Site 212 L. The amount of vehicle path curvature at the PC, and the indicated rate of spiraling, are typical of most observed vehicles.

Short Curve Vehicle Dynamics.--One interesting verification of the HVOSM driver model was provided by the field observations for Site 198, a short, right-hand curve. Observed vehicle paths were much less severe than would be predicted by the path vs. curve relationships derived previously. Inspection of the individual vehicle paths provided a clue as to what was different about this site. Because the curve length was so short, drivers literally did not have the opportunity to overshoot the highway curve radius. Instead, they spiraled into and out of the curve, with a minimum path radius generally greater than that of the highway. This same behavior was simulated previously in a run specifically designed to study short curve dynamics. At the time of the simulation it was hypothesized that very short curves produced additional dynamics due to rapid changes of roll angle, steering, etc. The results (see Table 21) produced the surprising (at the time) conclusion that vehicles generated less friction demand on very short curves. It was left to the field studies to verify and explain why this was so.

Knowledge Obtainable Exclusively From HVOSM

HVOSM has been proven to accurately simulate nominally critical vehicle behavior on curves. There are obvious cost and time advantages in simulating rather than studying vehicle dynamics in the field. Also, there is a wealth of information provided by HVOSM which could not be obtained in a field experiment such as was

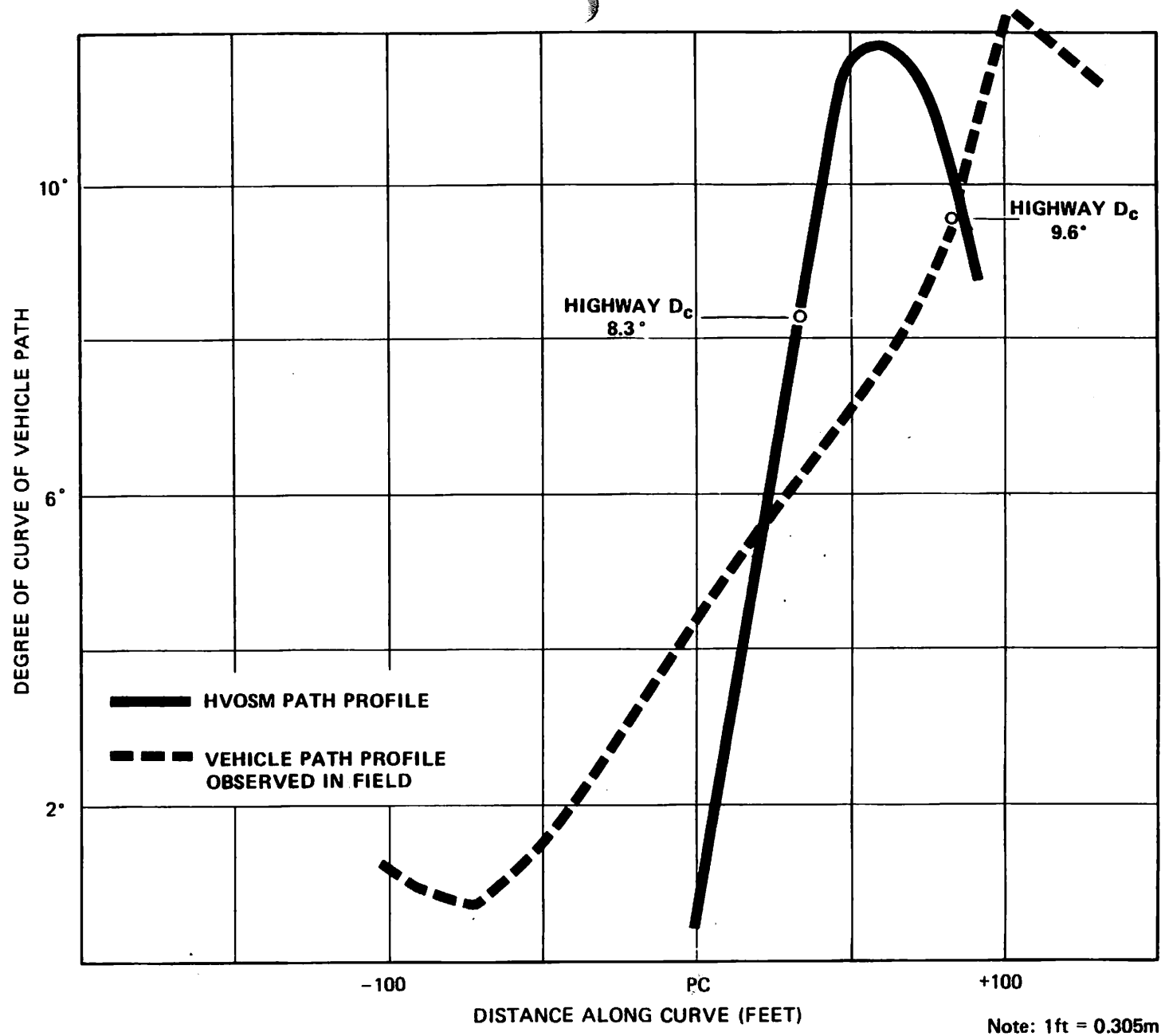


Figure 33. COMPARISON OF VEHICLE PATH TRANSITIONING BEHAVIOR FROM HVOSM AND VEHICLE TRAVERSAL STUDIES

performed for this research. Through simulation, not only can lateral acceleration be modeled, but also the distribution of lateral acceleration to the four tires. This is important in identifying thresholds of loss of control, which is dependent on friction demands on individual axles. Roll and steer angle data are also obtainable. Perhaps the most useful aspect of simulation is the ability to study dynamic effects on various vehicle types (e.g., trucks, semi-trailers, buses), or ranges of vehicle characteristics (e.g., front-wheel drive).

HVOSM has limited applications and usefulness, which are a function of the assumptions that are required to initiate the simulation. The assumptions generally relate to driver behavior. They include initial speed, acceleration/deceleration, and brake applications. HVOSM is also limited by its inability to address variable driver behavior as a function of changing environmental conditions.

Knowledge Obtainable Exclusively From Field Studies

The following discussion concerns crucial areas of vehicle operations for which actual observations of driver behavior are required. Knowledge obtained from field studies, combined with HVOSM or other simulations, can answer important questions about driver/vehicle behavior on highway curves.

Vehicle Speed Characteristics

Drivers' desired speed characteristics can only be determined by field measurements. The studies of speed and speed transition behavior showed that approach conditions and curvature have variable effects on desired speeds. Other factors such as weather or light conditions also can influence driver behavior. Field observations of vehicle speeds provide distributional data which enable more meaningful analysis of the criticality of a particular set of conditions. For example, one can simulate the vehicle dynamics resulting from a curve being "overdriven" by 10 mph (16 km/h). However, field measurements are required to determine what sets of conditions produce overdriving, and what percentage of the vehicles do in fact overdrive the curve.

Effect of Geometry on Path Behavior

Observed driver behavior in curve tracking is complex. Adaptation of the driver model in HVOSM to replicate this behavior requires extensive field data. One important design element which affects driving behavior is lane width. The vehicle traversal studies showed that drivers use the full lane to position their vehicles for spiraling into the curve. Given that this behavior is universal, one could expect highly variable spiraling behavior on 9- or 10-foot (2.7 or 3.0 m) lanes vs. 12- or 16-foot (3.7 or 4.9 m) lanes. Because the HVOSM driver model in its present form assumes that drivers desire to track the center of the lane, any effect of variable lane width on path would not be simulated.

Environmental Conditions

It is generally assumed that adverse weather conditions affect driving behavior. While changes in driving behavior are usually characterized in terms of lower speeds, it is possible that path-following behavior is also altered. Poor or limited visibility during rain, fog, or night time may have significant effects on the overshoot characteristics of drivers. Such effects could only be measured or estimated from actual observations of drivers.

Summary of HVOSM and Field Study Vehicle Dynamics

The total research effort demonstrated (1) the ability of HVOSM to predict vehicle dynamics across a range of curve conditions; and (2) the need to study actual vehicle behavior in order to assess the validity of the simulations. Both field studies and simulation work described driver behavior in a similar manner.

Spiraling Transitions

The studies of actual driver/vehicle behavior revealed that drivers spiral into horizontal curves. This spiraling behavior occurs at rates which vary with highway curvature. Simulated driver/vehicle behavior using HVOSM was generally similar in character. However, the simulated rate of spiraling was more severe than observed rates. This severe rate is attributed to the short probe length function which was a part of the HVOSM driver model.

Dynamic Overshoot

With selection of an appropriate, speed-sensitive probe length function, observed driver/vehicle overshoot can be simulated. The severity of overshoot can be related to a desired percentile of driver behavior. The HVOSM curve runs demonstrated the ability to then select a probe length that results in comparable simulation of path overshoot. In addition, the research validated the probe length function across the full range of speeds.

Vehicle Path

Simplifying assumptions in the driver model and the resulting overly severe simulated spiraling rates result in vehicle path simulations that differ from observed paths. The thrust of the research was to demonstrate nominally critical behavior in terms of maximum friction demand achieved under a range of conditions. HVOSM simulations successfully replicated friction demands calculated from observed vehicle paths. Moreover, the simulations were shown to produce similar minimum path radii as were observed in the field. However, the transient path behavior was not simulated.

Research Methodologies and Techniques

- (1) Determining the Accident Effects of Individual Elements - This study demonstrated the potential futility of using rigorous multivariate statistical procedures for determining the incremental accident effects of variable dimensions for individual highway elements. Not only is this endeavor sensitive to varying accident reporting levels and accuracy, but it requires an almost limitless study design and sample size to adequately represent all values of every geometric, operational and environmental element that create some variance in the accident experience.
- (2) Usefulness of General Statistical Techniques - The study demonstrated the usefulness of statistical techniques such as discriminant analysis. This technique successfully isolated those highway elements and their combinations which best distinguish high-accident locations from low-accident locations.
- (3) Usefulness of the HVOSM Techniques - The HVOSM simulation technique, using a 0.25 second driver preview of the highway ahead, was successful in replicating the maximum dynamic responses of extreme vehicle behavior on highway curves. This driver modeling, however, did not accurately replicate the way in which the maximum dynamic response was generated; i.e., the rate of vehicle spiraling was more severe than that observed in the field studies. This finding suggests a more complex model for driver preview may be appropriate in applying HVOSM to a study of highway curve traversal behavior. The driver's preview is apparently longer on the approach to the curve, and diminishes as the vehicle actually negotiates the highway curve.
- (4) Usefulness of Field Studies - The field observations of driver behavior at a limited number of highway curve sites demonstrated an effective means for identifying both general and critical driver behavior. With a broader range of sites, a more comprehensive study could include the operational effects of roadway width, shoulder width, advanced sight distance, and other elements.

Research Methodologies and Techniques

- (1) Determining the Accident Effects of Individual Elements - This study demonstrated the potential futility of using rigorous multivariate statistical procedures for determining the incremental accident effects of variable dimensions for individual highway elements. Not only is this endeavor sensitive to varying accident reporting levels and accuracy, but it requires an almost limitless study design and sample size to adequately represent all values of every geometric, operational and environmental element that create some variance in the accident experience.
- (2) Usefulness of General Statistical Techniques - The study demonstrated the usefulness of statistical techniques such as discriminant analysis. This technique successfully isolated those highway elements and their combinations which best distinguish high-accident locations from low-accident locations.
- (3) Usefulness of the HVOSM Techniques - The HVOSM simulation technique, using a 0.25 second driver preview of the highway ahead, was successful in replicating the maximum dynamic responses of extreme vehicle behavior on highway curves. This driver modeling, however, did not accurately replicate the way in which the maximum dynamic response was generated; i.e., the rate of vehicle spiraling was more severe than that observed in the field studies. This finding suggests a more complex model for driver preview may be appropriate in applying HVOSM to a study of highway curve traversal behavior. The driver's preview is apparently longer on the approach to the curve, and diminishes as the vehicle actually negotiates the highway curve.
- (4) Usefulness of Field Studies - The field observations of driver behavior at a limited number of highway curve sites demonstrated an effective means for identifying both general and critical driver behavior. With a broader range of sites, a more comprehensive study could include the operational effects of roadway width, shoulder width, advanced sight distance, and other elements.

REFERENCES

- (1) Roy Jorgensen Associates - "Cost and Safety Effectiveness of Highway Design Elements," National Cooperative Highway Research Program Report 197, 1978.
- (2) Kihlberg, K.K. and Tharp, K.J. - "Accident Rates as Related to Design Elements of Rural Highways," National Cooperative Highway Research Program Report 47, 1968.
- (3) Billion, C.E. and Stohner, W.R. - "A Detailed Study of Accidents as Related to Highway Shoulders in New York State," Highway Research Board Proceedings, 1957.
- (4) Babkov, V.F. - "Road Design and Traffic Safety," Traffic Engineering and Control, September 1968.
- (5) Coburn, T.M. - "The Relation Between Accidents and Layout on Rural Roads," International Road Safety & Traffic Review, Volume X Number 4 (Autumn 1962).
- (6) Taylor, W.C. and Foody, T.J. - Curve Delineation and Accidents, Ohio Department of Highways, 1966.
- (7) Raff, M.S. - "Interstate Highway Accident Study," Highway Research Board Bulletin No. 74, 1953.
- (8) Dart, O.K. and Mann, L. - "Relationship of Rural Highway Geometry to Accident Rates in Louisiana," Highway Research Board Record No. 312, 1970.
- (9) Stohner, W.R. - "Relation of Highway Accidents to Shoulder Width on Two-lane Rural Highways in New York State," - paper presented at 35th Annual Meeting of the Highway Research Board, 1965.
- (10) Gupta, R.C. and Jain, R.P. - "Effect of Certain Roadway Characteristics on Accident Rates for Two-lane, Two-way Roads in Connecticut," Transportation Research Board Record No. 541, 1975.
- (11) Sparks, J.W. - "The Influence of Highway Characteristics on Accident Rates," Public Works, March 1968.
- (12) Zegeer, C.V. and Mayes, J.G. - Cost-effectiveness of Lane and Shoulder Widening of Rural, Two-lane Roads in Kentucky, Kentucky Department of Transportation, 1979.
- (13) Schoppert, D.W. - "Predicting Traffic Accidents from Roadway Elements of Rural Two-lane Highways with Gravel Shoulders," Highway Research Board Bulletin No. 158, 1957.
- (14) Perkins, E.T. - "Relationship of Accident Rate to Highway Shoulder Width," Highway Research Board Bulletin No. 151, 1957.

- (15) Taragin, A. and Eckhardt, H.G. - "Effect of Shoulders on Speed and Lateral Placement of Motor Vehicles," Highway Research Board Proceedings 32, 1953.
- (16) Taragin, A. - "Role of Highway Shoulders in Traffic Operation," Highway Research Board Bulletin No. 151, 1957.
- (17) Foody, T.J. and Long, M.D. - The Identification of Relationships Between Safety and Roadside Obstructions, Ohio Department of Transportation, January 1974.
- (18) Cirillo, J.P. - "Interstate System Accident Research--Study II," Highway Research Board Record No. 188, 1967.
- (19) Agent, K.R. and Dean, R.C. - "Relationships Between Roadway Geometrics and Accidents," Transportation Research Board Record No. 541, 1975.
- (20) Glennon, J.C. and Wilton, C.J. - Effectiveness of Roadside Safety Improvements: A Methodology for Determining the Safety Effectiveness of Improvements on All Classes of Highways, Federal Highway Administration, November 1974.
- (21) DeLeys, N.J. - Safety Aspects of Roadside Cross-Section Design, Calspan Corp., February 1975.
- (22) Wright, P.H. and Zador, P. - "A Study of Fatal Rollover Crashes in Georgia," paper presented at Transportation Research Board Annual Meeting, January 1981.
- (23) Hall, J.W. and Zador, P. - "A Study of Fatal Overturning Crash Sites," paper presented at Transportation Research Board Annual Meeting, January 1981.
- (24) Graham, J.L. and Harwood, D.W. - "Effectiveness of Clear Recovery Zones," National Cooperative Highway Research Program Report 247, May 1982.
- (25) Cleveland, D.E. and Kitamura, R. - "Macroscopic Modeling of Two-lane Rural Road Accidents," paper presented at Transportation Research Board Annual Meeting, January 1978.
- (26) U.S. Department of Transportation - Highway Statistics 1976, Report No. FHWA HP-HS-76, Table SM-15, January 1978.
- (27) Long, L.H. ed., The World Almanac 1972 edition, Newspaper Enterprise Association, Inc.
- (28) Nie, N.H. et al. - Statistical Package for the Social Sciences, Second Edition, McGraw Hill, Inc., 1975.
- (29) Glennon, J.C. "Roadside Safety Improvement Programs on Freeways--A Cost-effectiveness Priority Approach," National Cooperative Highway Research Program Report 148, 1974.
- (30) McHenry, R.R. and DeLeys, N.J. - Vehicle Dynamics in Single Vehicle Accidents--Validation and Extensions of a Computer Simulation, Calspan Corp., CAL Report No. VJ-2251-3, December 1968.

- (31) Glennon, J.C. et al. - HVOSM Studies of Cross-slope Breaks on Highway Curves, Federal Highway Administration Report No. FHWA RD-82/054, May 1982.
- (32) American Association of State Highway and Transportation Officials "A Policy on Geometric Design of Highways and Streets," National Cooperative Highway Research Program Project 20-7, Task 14, Review Draft No. 2, December 1979.
- (33) Glennon, J.C. and Weaver, G.D. - "Highway Curve Design for Safety Vehicle Operations," Highway Research Board Record No. 390, 1972.
- (34) Leisch, J.E. and Leisch, J.P. - "New Concepts in Design Speed Application," paper presented at Transportation Research Board Annual Meeting, January 1977.
- (35) American Association of State Highway Officials, A Policy on Geometric Design of Rural Highways, 1965.
- (36) Wright, P.H. and Zador, P. - "A Study of Fatal Rollover Crashes in Georgia," paper presented at Transportation Research Board Annual Meeting, January 1981.
- (37) Hall, J.W. and Zador, P. - "A Survey of Fatal Overturning Crash Sites," paper presented at Transportation Research Board Annual Meeting, January 1981.
- (38) Neuman, T.R. et al. - Stopping Sight Distance--An Operational and Cost-Effectiveness Analysis Federal Highway Administration Unpublished Report, July 1982.
- (39) Klein, R.H. et al. - Influence of Roadway Disturbances on Vehicle Handling, Volume I: Summary Report, National Highway Traffic Safety Administration Report No. DOT HS-802 210, February 1977.
- (40) American Association of State Highway and Transportation Officials, A Manual on User Benefit Analysis of Highway and Bus-Transit Improvements, 1977.
- (41) Faigin, B.M. - 1975 Societal Costs of Motor Vehicle Accidents, National Highway Traffic Safety Administration, December 1976.
- (42) Federal Highway Administration, Fatal and Injury Accident Rates on Federal-aid and Other Highway Systems/1975.
- (43) Federal Highway Administration, Highway Statistics (1976-1980 editions)
- (44) McMahon, L.A. - 1981 Dodge Guide to Public Works and Heavy Construction Costs, McGraw Hill Inc.
- (45) Bali, S. et al. - Cost-effectiveness and Safety of Alternative Roadway Delineation Treatments For Rural Two-lane Highways, Federal Highway Administration Report RD-78-51, April 1978.

- (46) McFarland, W.F. et al. - Assessment of Techniques for Cost-effectiveness of Highway Accident Countermeasures, Federal Highway Administration Report RD-79-53, January 1979.
- (47) Segal, D.J. - Highway-Vehicle-Object-Simulation Model - 1976. Contract: DOT-FH-11-8265, February 1976, Volumes 1-4, NTIS# PB267401-PB267404.
- (48) Schuring, D.J. et al - The Influence of Tire Properties on Passenger Vehicle Handling. Volumes I-V. Contract: DOT-HS-053-3-727, June 1974.
- (49) Segal, D.J and Ranney, T.A. - Evaluation of Horizontal Curve Requirements, Final Report No. FHWA-RD-79-48, October 1978.

APPENDIX D

HVOSM CURVE RUN DOCUMENTATION

HVOSM Input Parameters

The Roadside Design (RD2) version of HVOSM, as documented in Reference (49) was used for the present research. Some modifications of the simulation program were incorporated for this application as discussed later in this Appendix.

The specific vehicle that was simulated in the curve studies was a 1971 Dodge Coronet 4-door sedan. The inputs for the simulated vehicle were obtained from Appendix D of Reference (48). An input data deck listing and a corresponding parameter list of the inputs are presented in Figures 49 and 50.

HVOSM Curve Study Setup Procedure

The procedure to set up an HVOSM curve run for the present research effort was as follows:

- (1) Analytically determine the extent of roadway required to meet the requirements of the particular run (i.e., roadway radius and length).
- (2) Set up and run a Terrain Table Generator (TTG) run based on roadway specifications.
- (3) Insert TTG run output "cards" into HVOSM data deck.
- (4) Set up and insert HVOSM Driver Model Input cards per run specification into HVOSM data deck.
- (5) Perform the simulation run.

The "cards" referred to were actually disk files and all insertions and manipulations of "card" decks were actually done interactively on disk files. The use of disk files enabled the rapid manipulation of "card" decks for each simulation run, as well as retention of the card deck for each run in a single partitioned disk data set.

MCI-JEL HVOSM CURVE STUDIES: RUN:MCS#18										0 100
0.0	4.97	0.010	0.010	70.0	0.0	0.0				0 101
0	0									0 102
	1									0 103
	1	1	1	1	1	1	1			0 104
1971 DODGE CORONET 4-DOOR SEDAN										0 200
8.43	0.51	0.82	3750.0	23000.0	23300.0	530.0	550.0			0 201
49.3	68.7	59.8	61.8	0.0	47.0					0 202
0.0	-14.0	0.0	-68.7	-30.9	10.1	10.82	10.68			0 203
108.0	189.0	600.0	588.0	600.0	0.50	-2.40	2.1			0 204
120.0	324.0	600.0	864.0	600.0	0.50	-4.40	3.6			0 205
6.85	40.0	0.10	7.48	38.0	0.10					0 206
40400.0	-5100.	0.02								0 207
		0.559								0 208
-3.0	3.0	1.0								0 209
-0.43	-0.95	-1.22	-1.26	-0.98	-0.41	0.0				1 209
FIRESTONE RADIAL VI										0 300
1.0	1.0	1.0	1.0	6.0	0.25					0 301
1450.0	3.0	10.0	-37.0	13.2	3043.	.58	91435.	1.0		1 301
.78				13.2						0 302
210 M PATH, 5% BRAKING, PROBE 25%										0 400
0.0	5.0	1.0	0.0	0.0	1.0					0 401
-95.	-95.	-95.	-95.	-95.						1 401
1.0	1.0	1.0	0.05	.00905	0.000	0.0				0 402
4.0	100.	0.0	0.0	1.5708	120.					0 403
0.0	0.0	0.0	600.	-.6892	720.	-.6892	12000.			0 404
0.0	0.1	264.	0.0	0.5	400.	0.00380	0.000380			0 405
210 M RADIUS, 10% SE, 5% GRADE, 80 M RUNOFF, 20/80% DIST										0 500
-600.00	600.00	60.00	0.0	1200.00	60.00	0.0				0 501
6.00	9.00	12.00	13.73	15.46	17.19	18.92	20.65	22.38	1 501	
24.12	25.85	27.58	29.18	30.91	32.61	34.28	35.75	37.33	2 501	
38.85	40.39	41.88	0.0	0.0	0.0	0.0	0.0	0.0	3 501	
5.40	8.40	11.40	13.26	15.12	16.97	18.83	20.69	22.55	4 501	
24.40	26.26	28.12	29.86	31.71	33.54	35.33	36.94	38.65	5 501	
40.30	41.97	43.59	0.0	0.0	0.0	0.0	0.0	0.0	6 501	
4.80	7.80	10.80	12.78	14.77	16.75	18.74	20.72	22.71	7 501	
24.69	26.68	28.66	30.53	32.51	34.47	36.39	38.13	39.97	8 501	
41.75	43.55	45.31	0.0	0.0	0.0	0.0	0.0	0.0	9 501	
4.20	7.20	10.20	12.31	14.42	16.53	18.65	20.76	22.87	10 501	
24.98	27.09	29.20	31.21	33.31	35.40	37.45	39.33	41.31	11 501	
43.22	45.15	47.04	0.0	0.0	0.0	0.0	0.0	0.0	12 501	
3.60	6.60	9.60	11.84	14.08	16.32	18.55	20.79	23.03	13 501	
25.27	27.51	29.75	31.89	34.12	36.33	38.52	40.54	42.65	14 501	
44.70	46.76	48.79	0.0	0.0	0.0	0.0	0.0	0.0	15 501	
3.00	6.00	9.00	11.37	13.73	16.10	18.46	20.83	23.19	16 501	
25.56	27.92	30.29	32.57	34.93	37.27	39.59	41.75	44.00	17 501	
46.19	48.39	50.55	0.0	0.0	0.0	0.0	0.0	0.0	18 501	
2.40	5.40	8.40	10.89	13.38	15.88	18.37	20.86	23.35	19 501	
25.85	28.34	30.83	33.25	35.74	38.21	40.66	42.98	45.35	20 501	
47.69	50.02	52.33	0.0	0.0	0.0	0.0	0.0	0.0	21 501	
1.80	4.80	7.80	10.42	13.04	15.66	18.28	20.90	23.52	22 501	
26.13	28.75	31.37	33.94	36.55	39.15	41.73	44.20	46.72	23 501	
49.20	51.67	54.12	0.0	0.0	0.0	0.0	0.0	0.0	24 501	
1.20	4.20	7.20	9.95	12.69	15.44	18.18	20.93	23.68	25 501	
26.42	29.17	31.92	34.62	37.36	40.09	42.81	45.44	48.10	26 501	
50.72	53.34	55.92	0.0	0.0	0.0	0.0	0.0	0.0	27 501	
0.60	3.60	6.60	9.47	12.35	15.22	18.09	20.97	23.84	28 501	
26.71	29.58	32.46	35.31	38.18	41.04	43.89	46.68	49.48	29 501	
52.26	55.02	57.75	0.0	0.0	0.0	0.0	0.0	0.0	30 501	
0.0	3.00	6.00	9.00	12.00	15.00	18.00	21.00	24.00	31 501	

FIGURE 49. TYPICAL CARD IMAGE OF HVOSM INPUTS FOR HVOSM CURVE STUDY

27.00	30.00	33.00	36.00	38.99	41.99	44.97	47.93	50.88	32 501
53.80	56.71	59.59	0.0	0.0	0.0	0.0	0.0	0.0	33 501
-0.60	2.40	5.40	8.53	11.65	14.78	17.91	21.03	24.16	34 501
27.29	30.42	33.54	36.69	39.81	42.94	46.08	49.19	52.29	35 501
55.36	58.42	61.44	0.0	0.0	0.0	0.0	0.0	0.0	36 501
-1.20	1.80	4.80	8.05	11.31	14.56	17.82	21.07	24.32	37 501
27.58	30.83	34.08	37.39	40.63	43.89	47.20	50.45	53.71	38 501
56.93	60.14	63.31	0.0	0.0	0.0	0.0	0.0	0.0	39 501
-1.80	1.20	4.20	7.58	10.96	14.34	17.72	21.10	24.48	40 501
27.87	31.25	34.63	38.08	41.46	44.84	48.23	51.72	55.15	41 501
58.51	61.88	65.20	0.0	0.0	0.0	0.0	0.0	0.0	42 501
-2.40	0.60	3.60	7.11	10.62	14.12	17.63	21.14	24.65	43 501
28.15	31.66	35.17	38.78	42.28	45.80	49.46	53.00	56.59	44 501
60.11	63.64	67.11	0.0	0.0	0.0	0.0	0.0	0.0	45 501
-3.00	0.00	3.00	6.63	10.27	13.90	17.54	21.17	24.81	46 501
28.44	32.08	35.71	39.48	43.11	46.76	50.61	54.29	58.05	47 501
61.71	65.41	69.03	0.0	0.0	0.0	0.0	0.0	0.0	48 501
-3.60	-0.60	2.40	6.16	9.92	13.68	17.45	21.21	24.97	49 501
28.73	32.49	36.25	40.18	43.93	47.72	51.75	55.58	59.52	50 501
63.34	67.20	70.97	0.0	0.0	0.0	0.0	0.0	0.0	51 501
-4.20	-1.20	1.80	5.69	9.58	13.47	17.35	21.24	25.13	52 501
29.02	32.91	36.80	40.88	44.76	48.69	52.91	56.88	61.00	53 501
64.97	69.00	72.94	0.0	0.0	0.0	0.0	0.0	0.0	54 501
-4.80	-1.80	1.20	5.22	9.23	13.25	17.26	21.28	25.29	55 501
29.31	33.32	37.34	41.59	45.59	49.65	54.07	58.20	62.48	56 501
66.62	70.82	74.92	0.0	0.0	0.0	0.0	0.0	0.0	57 501
-5.40	-2.40	0.60	4.74	8.88	13.03	17.17	21.31	25.45	58 501
29.60	33.74	37.88	42.29	46.43	50.62	55.23	59.52	63.98	59 501
68.28	72.65	76.92	0.0	0.0	0.0	0.0	0.0	0.0	60 501
-6.00	-3.00	0.00	4.27	8.54	12.81	17.08	21.35	25.62	61 501
29.88	34.15	38.42	43.00	47.26	51.59	56.40	60.84	65.50	62 501
69.96	74.50	78.95	0.0	0.0	0.0	0.0	0.0	0.0	63 501
-600.00	600.00	60.00	1200.00	2400.00	60.00	0.0			0 502
41.88	43.38	44.81	46.26	47.63	49.01	50.31	51.61	52.85	1 502
54.05	55.20	56.31	57.36	58.36	59.30	60.18	61.01	61.77	2 502
62.48	63.10	63.67	0.0	0.0	0.0	0.0	0.0	0.0	3 502
43.59	45.21	46.78	48.34	49.85	51.35	52.78	54.21	55.57	4 502
56.89	58.16	59.39	60.56	61.68	62.75	63.75	64.69	65.57	5 502
66.39	67.12	67.81	0.0	0.0	0.0	0.0	0.0	0.0	6 502
45.31	47.06	48.76	50.45	52.09	53.71	55.28	56.82	58.30	7 502
59.76	61.15	62.51	63.80	65.04	66.23	67.35	68.41	69.40	8 502
70.34	71.19	71.99	0.0	0.0	0.0	0.0	0.0	0.0	9 502
47.04	48.92	50.75	52.58	54.35	56.10	57.79	59.47	61.08	10 502
62.66	64.17	65.66	67.07	68.44	69.74	70.99	72.17	73.28	11 502
74.33	75.31	76.22	0.0	0.0	0.0	0.0	0.0	0.0	12 502
48.79	50.80	52.77	54.72	56.63	58.51	60.34	62.14	63.88	13 502
65.59	67.23	68.84	70.38	71.87	73.30	74.67	75.97	77.21	14 502
78.37	79.47	80.49	0.0	0.0	0.0	0.0	0.0	0.0	15 502
50.55	52.69	54.80	56.89	58.93	60.94	62.90	64.83	66.71	16 502
68.55	70.32	72.06	73.72	75.34	76.89	78.39	79.81	81.17	17 502
82.46	83.68	84.82	0.0	0.0	0.0	0.0	0.0	0.0	18 502
52.33	54.61	56.85	59.07	61.25	63.40	65.50	67.56	69.57	19 502
71.54	73.44	75.31	77.10	78.85	80.53	82.15	83.69	85.18	20 502
86.59	87.93	89.19	0.0	0.0	0.0	0.0	0.0	0.0	21 502
54.12	56.54	58.92	61.28	63.60	65.88	68.12	70.31	72.46	22 502
74.56	76.60	78.59	80.52	82.40	84.20	85.95	87.63	89.24	23 502
90.77	92.23	93.61	0.0	0.0	0.0	0.0	0.0	0.0	24 502
55.92	58.49	61.01	63.51	65.97	68.39	70.76	73.09	75.38	25 502
77.61	79.79	81.92	83.98	85.99	87.92	89.80	91.60	93.34	26 502
94.99	96.58	98.08	0.0	0.0	0.0	0.0	0.0	0.0	27 502
57.75	60.45	63.12	65.76	68.36	70.92	73.44	75.91	78.33	28 502

FIGURE 49. TYPICAL CARD IMAGE OF HVOSM INPUTS FOR HVOSM CURVE STUDY (Continued)

80.70	83.02	85.28	87.47	89.61	91.68	93.69	95.62	97.49	29 502
99.27	100.98	102.61	0.0	0.0	0.0	0.0	0.0	0.0	30 502
59.59	62.44	65.25	68.03	70.78	73.48	76.14	78.75	81.31	31 502
83.82	86.28	88.67	91.01	93.28	95.49	97.63	99.69	101.68	32 502
103.60	105.44	107.19	0.0	0.0	0.0	0.0	0.0	0.0	33 502
61.44	64.44	67.40	70.33	73.22	76.07	78.87	81.62	84.33	34 502
86.98	89.57	92.11	94.58	96.99	99.33	101.61	103.81	105.93	35 502
107.97	109.94	111.82	0.0	0.0	0.0	0.0	0.0	0.0	36 502
63.31	66.48	69.57	72.65	75.69	78.68	81.63	84.53	87.38	37 502
90.17	92.91	95.59	98.20	100.75	103.23	105.63	107.97	110.22	38 502
112.40	114.50	116.51	0.0	0.0	0.0	0.0	0.0	0.0	39 502
65.20	68.51	71.76	75.00	78.18	81.33	84.42	87.47	90.46	40 502
93.40	96.28	99.10	101.86	104.55	107.17	109.71	112.18	114.57	41 502
116.89	119.11	121.26	0.0	0.0	0.0	0.0	0.0	0.0	42 502
67.11	70.57	73.98	77.37	80.70	84.00	87.24	90.44	93.58	43 502
96.67	99.70	102.66	105.56	108.39	111.15	113.84	116.45	118.97	44 502
121.42	123.78	126.06	0.0	0.0	0.0	0.0	0.0	0.0	45 502
69.03	72.65	76.22	79.76	83.25	86.70	90.10	93.45	96.74	46 502
99.97	103.15	106.26	109.31	112.28	115.19	118.01	120.76	123.43	47 502
126.01	128.51	130.92	0.0	0.0	0.0	0.0	0.0	0.0	48 502
70.97	74.76	78.48	82.18	85.82	89.43	92.98	96.48	99.93	49 502
103.32	106.65	109.90	113.10	116.22	119.27	122.24	125.13	127.94	50 502
130.66	133.29	135.84	0.0	0.0	0.0	0.0	0.0	0.0	51 502
72.94	76.88	80.76	84.62	88.43	92.19	95.90	99.56	103.17	52 502
106.70	110.19	113.59	116.94	120.20	123.41	126.51	129.56	132.50	53 502
135.37	138.14	140.82	0.0	0.0	0.0	0.0	0.0	0.0	54 502
74.92	79.03	83.08	87.09	91.07	94.98	98.86	102.67	106.44	55 502
110.12	113.77	117.32	120.83	124.24	127.59	130.85	134.03	137.12	56 502
140.13	143.05	145.87	0.0	0.0	0.0	0.0	0.0	0.0	57 502
76.92	81.20	85.41	89.59	93.73	97.81	101.86	105.81	109.75	58 502
113.59	117.39	121.10	124.76	128.32	131.82	135.23	138.57	141.80	59 502
144.96	148.02	150.98	0.0	0.0	0.0	0.0	0.0	0.0	60 502
78.95	83.38	87.78	92.12	96.43	100.66	104.89	109.00	113.10	61 502
117.10	121.06	124.92	128.74	132.46	136.11	139.68	143.16	146.55	62 502
149.84	153.05	156.15	0.0	0.0	0.0	0.0	0.0	0.0	63 502
-240.00	1440.00	120.00	2280.00	4680.00	120.00	0.0	0.0	0.0	0 503
86.59	89.19	91.48	93.43	95.04	96.28	97.15	97.62	97.68	1 503
97.33	98.30	99.81	101.13	102.28	103.23	103.98	104.55	104.92	2 503
105.13	105.18	105.02	0.0	0.0	0.0	0.0	0.0	0.0	3 503
94.99	98.08	100.85	103.27	105.34	107.02	108.32	109.21	109.68	4 503
109.75	111.44	112.96	114.30	115.44	116.39	117.14	117.72	118.09	5 503
118.30	118.30	118.14	0.0	0.0	0.0	0.0	0.0	0.0	6 503
103.60	107.19	110.44	113.35	115.88	118.02	119.75	121.06	121.95	7 503
122.90	124.61	126.15	127.49	128.64	129.58	130.34	130.91	131.27	8 503
131.48	131.47	131.28	0.0	0.0	0.0	0.0	0.0	0.0	9 503
112.40	116.51	120.27	123.66	126.67	129.28	131.46	133.21	134.51	10 503
136.07	137.81	139.35	140.71	141.86	142.81	143.57	144.11	144.49	11 503
144.66	144.66	144.46	0.0	0.0	0.0	0.0	0.0	0.0	12 503
121.42	126.06	130.33	134.23	137.73	140.81	143.44	145.64	147.37	13 503
149.28	151.04	152.61	153.96	155.11	156.06	156.82	157.36	157.74	14 503
157.90	157.87	157.68	0.0	0.0	0.0	0.0	0.0	0.0	15 503
130.66	135.84	140.65	145.06	149.05	152.62	155.73	158.38	160.57	16 503
162.53	164.31	165.88	167.24	168.39	169.35	170.09	170.65	171.01	17 503
171.16	171.12	170.92	0.0	0.0	0.0	0.0	0.0	0.0	18 503
140.13	145.87	151.22	156.15	160.66	164.72	168.32	171.42	173.82	19 503
175.82	177.60	179.19	180.56	181.71	182.67	183.41	183.97	184.30	20 503
184.44	184.42	184.17	0.0	0.0	0.0	0.0	0.0	0.0	21 503
149.84	156.15	162.05	167.53	172.57	177.13	181.22	184.80	187.12	22 503
189.13	190.94	192.53	193.90	195.07	196.01	196.76	197.31	197.64	23 503
197.77	197.73	197.49	0.0	0.0	0.0	0.0	0.0	0.0	24 503
159.80	166.70	173.18	179.21	184.78	189.87	194.46	198.21	200.45	25 503

FIGURE 49. TYPICAL CARD IMAGE OF HVOSM INPUTS FOR HVOSM CURVE STUDY (Continued)

202.49	204.31	205.91	207.29	208.46	209.40	210.15	210.68	211.00	26 503
211.14	211.06	210.81	0.0	0.0	0.0	0.0	0.0	0.0	27 503
170.04	177.54	184.60	191.21	197.33	202.95	208.04	211.55	213.83	28 503
215.89	217.72	219.33	220.71	221.89	222.83	223.58	224.10	224.40	29 503
224.53	224.46	224.15	0.0	0.0	0.0	0.0	0.0	0.0	30 503
180.56	188.67	196.33	203.51	210.19	216.36	221.98	224.94	227.24	31 503
229.32	231.16	232.78	234.17	235.34	236.30	237.03	237.54	237.86	32 503
237.95	237.86	237.53	0.0	0.0	0.0	0.0	0.0	0.0	33 503
191.34	200.09	208.37	216.15	223.41	230.14	235.83	238.37	240.69	34 503
242.79	244.65	246.28	247.68	248.84	249.80	250.52	251.02	251.33	35 503
251.44	251.29	250.88	0.0	0.0	0.0	0.0	0.0	0.0	36 503
202.42	211.83	220.75	229.15	237.02	244.31	249.28	251.85	254.20	37 503
256.31	258.18	259.82	261.21	262.40	263.34	264.06	264.57	264.85	38 503
264.93	264.76	264.32	0.0	0.0	0.0	0.0	0.0	0.0	39 503
213.84	223.93	233.51	242.54	250.99	258.86	262.75	265.36	267.73	40 503
269.86	271.75	273.40	274.80	275.99	276.93	277.63	278.14	278.42	41 503
278.45	278.21	277.78	0.0	0.0	0.0	0.0	0.0	0.0	42 503
225.62	236.38	246.60	256.27	265.35	273.40	276.28	278.92	281.32	43 503
283.47	285.37	287.03	288.45	289.62	290.55	291.26	291.75	292.02	44 503
292.03	291.76	291.30	0.0	0.0	0.0	0.0	0.0	0.0	45 503
240.00	2400.00	127.06	4560.00	6000.00	120.00	0.0			0 504
157.87	157.68	157.29	156.74	155.97	154.95	153.80	152.48	151.15	1 504
149.34	147.65	145.67	143.25	0.0	0.0	0.0	0.0	0.0	2 504
171.90	171.70	171.31	170.69	169.90	168.85	167.68	166.41	164.79	3 504
163.10	161.38	159.08	157.16	0.0	0.0	0.0	0.0	0.0	4 504
185.98	185.73	185.33	184.69	183.79	182.75	181.69	180.30	178.62	5 504
177.03	174.87	172.79	170.82	0.0	0.0	0.0	0.0	0.0	6 504
200.08	199.84	199.37	198.64	197.79	196.72	195.62	194.10	192.61	7 504
190.84	188.64	186.78	184.21	0.0	0.0	0.0	0.0	0.0	8 504
214.23	213.95	213.45	212.70	211.78	210.83	209.43	208.05	206.48	9 504
204.42	202.69	200.52	197.90	0.0	0.0	0.0	0.0	0.0	10 504
228.40	228.08	227.50	226.75	225.84	224.85	223.42	222.05	220.15	11 504
218.28	216.50	214.03	211.54	0.0	0.0	0.0	0.0	0.0	12 504
242.59	242.26	241.65	240.87	240.04	238.77	237.55	236.04	234.08	13 504
232.42	230.06	227.72	225.26	0.0	0.0	0.0	0.0	0.0	14 504
256.84	256.41	255.81	255.14	254.03	252.85	251.58	249.72	248.27	15 504
246.06	243.91	241.52	239.31	0.0	0.0	0.0	0.0	0.0	16 504
271.06	270.67	270.03	269.33	268.19	267.07	265.45	264.03	262.24	17 504
259.98	257.70	255.62	252.63	0.0	0.0	0.0	0.0	0.0	18 504
285.38	284.93	284.39	283.43	282.48	281.22	279.55	278.08	275.98	19 504
273.87	271.89	269.46	266.43	0.0	0.0	0.0	0.0	0.0	20 504
299.72	299.36	298.70	297.70	296.70	295.21	293.90	291.94	289.98	21 504
287.85	285.80	282.84	280.59	0.0	0.0	0.0	0.0	0.0	22 504
314.13	313.73	312.94	312.09	310.78	309.62	307.84	306.04	304.03	23 504
302.13	299.33	297.15	294.39	0.0	0.0	0.0	0.0	0.0	24 504
328.66	328.05	327.40	326.27	325.07	323.87	322.03	320.10	318.36	25 504
315.74	313.30	311.04	308.14	0.0	0.0	0.0	0.0	0.0	26 504
343.17	342.52	341.82	340.65	339.60	337.93	336.21	334.55	332.47	27 504
329.79	327.65	324.86	321.90	0.0	0.0	0.0	0.0	0.0	28 504
357.62	357.11	356.14	355.25	353.77	352.22	350.48	348.75	346.25	29 504
344.22	341.55	338.72	335.76	0.0	0.0	0.0	0.0	0.0	30 504
372.30	371.54	370.66	369.72	368.19	366.58	364.98	362.56	360.75	31 504
358.21	355.58	352.67	350.13	0.0	0.0	0.0	0.0	0.0	32 504
386.95	386.15	385.38	384.05	382.65	381.16	378.97	377.21	374.84	33 504
372.33	369.56	367.00	363.85	0.0	0.0	0.0	0.0	0.0	34 504
401.54	400.96	399.82	398.57	397.27	395.28	393.68	391.53	389.06	35 504
386.43	384.02	380.94	377.76	0.0	0.0	0.0	0.0	0.0	36 504
1.0	1.0	1.0	1.0						0 506
	100 KPH								0 600
0.57	-2.86	90.	0.0	0.0	0.0				0 601
0.0	120.	-17.3	1056.						0 602
0.0	0.0	0.0	0.0						0 603
									09999

FIGURE 49. TYPICAL CARD IMAGE OF HVOSM INPUTS FOR HVOSM CURVE STUDY (Continued)

MCI-JEL HVOSM CURVE STUDIES: RUN:MCS#18
 1971 DODGE CORONET 4-DOOR SEDAN FIRESTONE RADIAL VI
 210 M RADIUS, 10% SE, 5% GRADE, 80 M RUNOFF 100 KPH

10/05/81
 210 M PATH, 5% BRAKING, PROBE 25%

274

PROGRAM CONTROL DATA	
START TIME	TO = 0.0 SEC
END TIME	T1 = 4.9700 SEC
INTEGRATION INCREMENT	DTCOMP = 0.0100 SEC
INTEGRATION MODE	MODE = 1 (0-VARIABLE STEP ADAMS-MOULTON -1- RUNGA-KUTTA 2- FIXED STEP ADAMS-MOULTON)
PRINT INTERVAL	DTPRNT = 0.0100 SEC
SUSPENSION OPTION	ISUS = 0 (0- INDEPENDENT FRONT SUSPENSION, SOLID REAR AXLE -1- INDEPENDENT FRONT AND REAR SUSPENSION 2- SOLID FRONT AND REAR AXLES 0- NO CURB, NO STEER DEGREE OF FREEDOM -1- CURB -1-STEER DEGREE OF FREEDOM, NO CURB)
CURB/STEER OPTION	INDCRB = 0
CURB INTEGRATION INCR.	DELTC = 0.0 SEC
BARRIER OPTION	INDB = 0 (0- NO BARRIER 1- RIGID BARRIER, FINITE VERT. DIM. 2- " " " " INFINITE " " 3- DEFORM. " " FINITE " " 4- " " " " INFINITE " ")
BARRIER INTEGRATION INCR.	DELTB = 0.0 SEC

INITIAL CONDITIONS					
SPRUNG MASS C.G. POSITION	XCOP = 0.0 INCHES	SPRUNG MASS LINEAR VELOCITY	UO = 1056.00 IN/SEC		
	YCOP = 120.00 INCHES		VO = 0.0 IN/SEC		
	ZCOP = -17.30 INCHES		WO = 0.0 IN/SEC		
SPRUNG MASS ORIENTATION	PHIO = 0.57 DEGREES	SPRUNG MASS ANGULAR VELOCITY	PO = 0.0 DEG/SEC		
	THETAO = -2.86 DEGREES		QO = 0.0 DEG/SEC		
	PSIO = 90.00 DEGREES		RO = 0.0 DEG/SEC		
UNSPRUNG MASS POSITIONS	DEL10 = 0.0 INCHES	UNSPRUNG MASS VELOCITIES	DEL100 = 0.0 IN/SEC		
	DEL20 = 0.0 INCHES		DEL200 = 0.0 IN/SEC		
	DEL30 = 0.0 INCHES		DEL300 = 0.0 IN/SEC		
STEER ANGLE	PHIRO = 0.0 DEGREES	STEER VELOCITY	PHIROD = 0.0 DEG/SEC		
	PSIFIO = 0.0 DEGREES		PSIFDO = 0.0 DEG/SEC		

FIGURE 50. INPUT PARAMETER LISTING FOR "TYPICAL" HVOSM CURVE RUN

MCI-JEL HVOSM CURVE STUDIES: RUN:HCS#18
 1971 DODGE CORONET 4-DOOR SEDAN FIRESTONE RADIAL VI
 210 M RADIUS, 10% SE, 5% GRADE, 80 M RUNOFF 100 KPH

10/05/81
 210 M PATH, 5% BRAKING, PROBE 25%

FRONT WHEEL CAMBER VS SUSPENSION DEFLECTION		REAR WHEEL CAMBER VS SUSPENSION DEFLECTION		FRONT HALF-TRACK CHANGE VS SUSPENSION DEFLECTION		REAR HALF-TRACK CHANGE VS SUSPENSION DEFLECTION	
DELTA F INCHES	PHIC DEGREES	DELTA R NOT USED	PHIR C NOT USED	DELTA F INCHES	DTH F INCHES	DELTA R NOT USED	DTH R NOT USED
-3.00	-0.43	-3.00	0.0	-3.00	0.0	-3.00	0.0
-2.00	-0.95	-2.00	0.0	-2.00	0.0	-2.00	0.0
-1.00	-1.22	-1.00	0.0	-1.00	0.0	-1.00	0.0
0.0	-1.26	0.0	0.0	0.0	0.0	0.0	0.0
1.00	-0.98	1.00	0.0	1.00	0.0	1.00	0.0
2.00	-0.41	2.00	0.0	2.00	0.0	2.00	0.0
3.00	0.0	3.00	0.0	3.00	0.0	3.00	0.0

DRIVER CONTROL TABLES

T SEC	PSIF DEG	TOF LB-FT	TOR LB-FT	T SEC	PSIF DEG	TOF LB-FT	TOR LB-FT	T SEC	PSIF DEG	TOF LB-FT	TOR LB-FT	T SEC	PSIF DEG	TOF LB-FT	TOR LB-FT
0.0	0.0	0.0	-95.0	2.000	0.0	0.0	-95.0	4.000	0.0	0.0	-95.0				
1.000	0.0	0.0	-95.0	3.000	0.0	0.0	-95.0	5.000	0.0	0.0	0.0				

TIRE DATA

		RF	LF	RR	LR	
TIRE LINEAR SPRING RATE	AKT	=	1450.000	1450.000	1450.000	1450.000 LB/IN
DEFL. FOR INCREASED RATE	SIGT	=	3.000	3.000	3.000	3.000 INCHES
SPRING RATE INCREASING FACTOR	XLAMT	=	10.000	10.000	10.000	10.000
	A0	=	-37.000	-37.000	-37.000	-37.000
	A1	=	13.200	13.200	13.200	13.200
SIDE FORCE COEFFICIENTS	A2	=	3043.000	3043.000	3043.000	3043.000
	A3	=	0.580	0.580	0.580	0.580
	A4	=	91435.000	91435.000	91435.000	91435.000
TIRE OVERLOAD FACTOR	OMEGT	=	1.000	1.000	1.000	1.000
TIRE UNDEFLECTED RADIUS	RW	=	13.200	13.200	13.200	13.200 INCHES
TIRE / GROUND FRICTION COEF.	AMU	=	0.780	0.780	0.780	0.780

NO ANTI-PITCH TABLES

FIGURE 50. INPUT PARAMETER LISTING FOR "TYPICAL" HVOSM CURVE RUN (Continued)

MCI-JEL HVOSM CURVE STUDIES: RUN:HCS#18
 1971 DODGE CORONET 4-DOOR SEDAN FIRESTONE RADIAL VI
 210 M RADIUS, 10% SE, 5% GRADE, 80 M RUNOFF 100 KPH

10/05/81
 210 M PATH, 5% BRAKING, PROBE 25%

SPRUNG MASS	XMS	=	8.430 LB-SEC**2/IN
FRONT UNSPRUNG MASS	XMUF	=	0.510 LB-SEC**2/IN
REAR UNSPRUNG MASS	XMUR	=	0.820 LB-SEC**2/IN
X MOMENT OF INERTIA	XIX	=	3760.000 LB-SEC**2-IN
Y MOMENT OF INERTIA	XIY	=	23000.000 LB-SEC**2-IN
Z MOMENT OF INERTIA	XIZ	=	23300.000 LB-SEC**2-IN
XZ PRODUCT OF INERTIA	XIXZ	=	530.000 LB-SEC**2-IN
FRONT AXLE MOMENT OF INERTIA	XIF	=	0.0 NOT USED
REAR AXLE MOMENT OF INERTIA	XIR	=	550.000 LB-SEC**2-IN
GRAVITY	G	=	386.400 IN/SEC**2

ACCELEROMETER 1 POSITION	X1	=	0.0 INCHES
	Y1	=	-14.00 INCHES
	Z1	=	0.0 INCHES
ACCELEROMETER 2 POSITION	X2	=	-68.70 INCHES
	Y2	=	-30.90 INCHES
	Z2	=	10.10 INCHES

FRONT WHEEL X LOCATION	A	=	49.300 INCHES
REAR WHEEL X LOCATION	B	=	68.700 INCHES
FRONT WHEEL Z LOCATION	ZF	=	10.820 INCHES
REAR WHEEL Z LOCATION	ZR	=	10.680 INCHES
FRONT WHEEL TRACK	TF	=	59.800 INCHES
REAR WHEEL TRACK	TR	=	61.800 INCHES
FRONT ROLL AXIS	RHOF	=	0.0 NOT USED
REAR ROLL AXIS	RMO	=	0.0 INCHES
FRONT SPRING TRACK	TSF	=	0.0 NOT USED
REAR SPRING TRACK	TS	=	47.000 INCHES

FRONT AUX ROLL STIFFNESS	RF	=	40400.00 LB-IN/RAD
REAR AUX ROLL STIFFNESS	RR	=	-5100.00 LB-IN/RAD
REAR ROLL-STEER COEF.	AKRS	=	0.0200 RAD/RAD
	AKDS	=	0.0 NOT USED
REAR DEFL-STEER COEFS.	AKDS1	=	0.0 NOT USED
	AKDS2	=	0.0 NOT USED
	AKDS3	=	0.0 NOT USED

275

S T E E R I N G S Y S T E M			
MOMENT OF INERTIA	XIPS	=	0.0 LB-SEC**2-IN
COULOMB FRICTION TORQUE	CPSP	=	0.0 LB-IN
FRICTION LAG	EPSP	=	0.0 RAD/SEC
ANGULAR STOP RATE	AKPS	=	0.0 LB-IN/RAD
ANGULAR STOP POSITION	OMGPS	=	0.559 RADIANS
PNEUMATIC TRAIL	XPS	=	0.0 INCHES

FRONT SUSPENSION

SUSPENSION RATE	AKF	=	105.000 LB/IN
COMPRESSION STOP COEFS.	AKFC	=	189.000 LB/IN
	AKFCP	=	600.000 LB/IN**3
EXTENSION STOP COEFS.	AKFE	=	588.000 LB/IN
	AKFEP	=	600.000 LB/IN**3
COMPRESSION STOP LOCATION	OMEGFC	=	-2.400 INCHES
EXTENSION STOP LOCATION	OMEGFE	=	2.100 INCHES
STOP ENERGY DISSIPATION FACTOR	XLAMF	=	0.500
VISCOUS DAMPING COEF.	CF	=	6.850 LB-SEC/IN
COULOMB FRICTION	CFP	=	40.000 LB
FRICTION LAG	EPSF	=	0.100 IN/SEC

REAR SUSPENSION

AKR	=	120.000 LB/IN
AKRC	=	324.000 LB/IN
AKRCP	=	600.000 LB/IN**3
AKRE	=	864.000 LB/IN
AKREP	=	600.000 LB/IN**3
OMEGRC	=	-4.400 INCHES
OMEGRE	=	3.600 INCHES
XLAMR	=	0.500
CR	=	7.480 LB-SEC/IN
CRP	=	38.000 LB
EPSR	=	0.100 IN/SEC

FIGURE 50. INPUT PARAMETER LISTING FOR "TYPICAL" HVOSM CURVE RUN (Continued)

MCI-JEL HVOSM CURVE STUDIES: RUN:HCS#18
 1971 DODGE CORONET 4-DOOR SEDAN FIRESTONE RADIAL VI
 210 M RADIUS, 10% SE, 5% GRADE, 80 M RUNOFF 100 KPH

10/05/81
 210 M PATH, 5% BRAKING, PROBE 25%

PATH DESCRIPTORS	IPATH	=	1
NUMBER OF PATH DESCRIPTORS	KLI	=	4
NUMBER OF POINTS ON PATH	NPTS	=	100
DISTANCE BETWEEN POINTS	DELL	=	120.000 INCHES
COORDINATES OF 1ST PATH POINTS:	XINIT	=	0.0 INCHES
	YINIT	=	0.0 INCHES
INITIAL ROADWAY HEADING	PSA	=	90.00 DEGREES

PATH CURVATURE DESCRIPTORS:

DEGREE OF CURVATURE	DI(1)	=	0.0 DEGREES
DISTANCE ALONG PATH	RLI(1)	=	0.0 INCHES

DEGREE OF CURVATURE	DI(1)	=	0.0 DEGREES
DISTANCE ALONG PATH	RLI(1)	=	600.00 INCHES

DEGREE OF CURVATURE	DI(1)	=	-8.2704 DEGREES
DISTANCE ALONG PATH	RLI(1)	=	720.00 INCHES

DEGREE OF CURVATURE	DI(1)	=	-8.2704 DEGREES
DISTANCE ALONG PATH	RLI(1)	=	12000.00 INCHES

WAGON TONGUE STEER DESCRIPTORS	IWAGN	=	1
INITIAL PROBE SAMPLE TIME	TPRB	=	0.0 SECONDS
TIME INCREMENT BETWEEN SAMPLES	OPRB	=	0.100 SECONDS
LENGTH OF PROBE	PLGTH	=	284.00 INCHES
MINIMUM ACCEPTABLE ERROR	PMIN	=	0.0 INCHES
MAXIMUM OCCUPANT ACCELERATION	PMAX	=	0.500 G-UNITS
STEER CORRECTION FACTOR	PGAIN	=	.0038000 RAD/IN
STEER CORRECTION DAMPING FACTOR	OGAIN	=	.0003800 RAD-SEC/IN
MAXIMUM STEERING WHEEL RATE	PSIFD	=	400.000 DEG/SEC

FILTER DESCRIPTORS	IFILT	=	1
TIME LAG OF FILTER	TIL	=	0.050000 SECONDS
TIME LEAD OF FILTER	TI	=	0.009050 SECONDS
TIME DELAY OF FILTER	TAUF	=	0.0 SECONDS

FIGURE 50. INPUT PARAMETER LISTING FOR "TYPICAL" HVOSM CURVE RUN (Continued)

MCI-JEL HVOSM CURVE STUDIES: RUN:HCS#18
 1971 DODGE CORONET 4-DOOR SEDAN FIRESTONE RADIAL VI
 210 M RADIUS, 10% SE, 5% GRADE, 80 M RUNOFF 100 KPH

10/05/81
 210 M PATH, 5% BRAKING, PROBE 25%

N	PATH COORDINATES		TANGENT VECTORS		DEGREE OF CURVATURE
	X(N) (FT)	Y(N) (FT)	DX(N) (DEG)	DY(N) (DEG)	D(N) (DEG)
1	0.0	0.0	90.000	90.000	0.0
2	-0.000	10.000	90.000	90.000	0.0
3	-0.000	20.000	90.000	90.000	0.0
4	-0.000	30.000	90.000	90.000	0.0
5	-0.000	40.000	90.000	90.000	0.0
6	-0.000	50.000	90.000	90.000	0.0
7	-0.000	60.000	90.000	90.000	-8.270
8	0.072	70.000	89.173	89.173	-8.270
9	0.288	79.997	88.346	88.346	-8.270
10	0.649	89.991	87.519	87.519	-8.270
11	1.154	99.978	86.692	86.692	-8.270
12	1.803	109.957	85.865	85.865	-8.270
13	2.596	119.925	85.038	85.038	-8.270
14	3.533	129.881	84.211	84.211	-8.270
15	4.613	139.823	83.384	83.384	-8.270
16	5.837	149.747	82.557	82.557	-8.270
17	7.204	159.653	81.730	81.730	-8.270
18	8.714	169.539	80.903	80.903	-8.270
19	10.366	179.401	80.076	80.076	-8.270
20	12.161	189.239	79.249	79.249	-8.270
21	14.097	199.049	78.422	78.421	-8.270
22	16.175	208.831	77.594	77.594	-8.270
23	18.394	218.581	76.767	76.767	-8.270
24	20.753	228.299	75.940	75.940	-8.270
25	23.252	237.981	75.113	75.113	-8.270
26	25.891	247.627	74.286	74.286	-8.270
27	28.668	257.233	73.459	73.459	-8.270
28	31.584	266.798	72.632	72.632	-8.270
29	34.638	276.320	71.805	71.805	-8.270
30	37.829	285.797	70.978	70.978	-8.270
31	41.156	295.227	70.151	70.151	-8.270
32	44.619	304.608	69.324	69.324	-8.270
33	48.218	313.938	68.497	68.497	-8.270
34	51.950	323.215	67.670	67.670	-8.270
35	55.816	332.437	66.843	66.843	-8.270
36	59.815	341.603	66.016	66.016	-8.270
37	63.945	350.709	65.189	65.189	-8.270
38	68.207	359.755	64.362	64.362	-8.270
39	72.598	368.739	63.535	63.535	-8.270
40	77.119	377.658	62.708	62.708	-8.270
41	81.768	386.511	61.881	61.881	-8.270
42	86.545	395.295	61.054	61.054	-8.270
43	91.448	404.011	60.227	60.227	-8.270
44	96.476	412.654	59.400	59.399	-8.270
45	101.628	421.224	58.573	58.572	-8.270
46	106.903	429.719	57.745	57.745	-8.270
47	112.301	438.137	56.918	56.918	-8.270
48	117.819	446.476	56.091	56.091	-8.270
49	123.457	454.734	55.264	55.264	-8.270
50	129.214	462.910	54.437	54.437	-8.270

FIGURE 50. INPUT PARAMETER LISTING FOR "TYPICAL"
 HVOSM CURVE RUN (Continued)

MCI-JEL HVOSM CURVE STUDIES: RUN:HCS#18
 1971 DODGE CORONET 4-DOOR SEDAN FIRESTONE RADIAL VI
 210 M RADIUS, 10% SE, 5% GRADE, 80 M RUNOFF 100 KPH

10/05/81
 210 M PATH, 5% BRAKING, PROBE 25%

N	PATH COORDINATES		TANGENT VECTORS		DEGREE OF
	X(N) (FT)	Y(N) (FT)	DX(N) (DEG)	DY(N) (DEG)	CURVATURE D(N) (DEG)
51	135.088	471.002	53.610	53.610	-8.270
52	141.079	479.009	52.783	52.783	-8.270
53	147.184	486.928	51.956	51.956	-8.270
54	153.403	494.758	51.129	51.129	-8.270
55	159.735	502.498	50.302	50.302	-8.270
56	166.177	510.145	49.475	49.475	-8.270
57	172.729	517.699	48.648	48.648	-8.270
58	179.390	525.157	47.821	47.821	-8.270
59	186.157	532.519	46.994	46.994	-8.270
60	193.030	539.781	46.167	46.167	-8.270
61	200.007	546.944	45.340	45.340	-8.270
62	207.087	554.005	44.513	44.513	-8.270
63	214.268	560.964	43.686	43.686	-8.270
64	221.549	567.818	42.859	42.859	-8.270
65	228.927	574.566	42.032	42.032	-8.270
66	236.403	581.207	41.205	41.205	-8.270
67	243.973	587.740	40.378	40.377	-8.270
68	251.637	594.162	39.551	39.550	-8.270
69	259.393	600.474	38.724	38.723	-8.270
70	267.239	606.672	37.896	37.896	-8.270
71	275.174	612.757	37.069	37.069	-8.270
72	283.196	618.726	36.242	36.242	-8.270
73	291.303	624.579	35.415	35.415	-8.270
74	299.494	630.315	34.588	34.588	-8.270
75	307.767	635.931	33.761	33.761	-8.270
76	316.120	641.428	32.934	32.934	-8.270
77	324.551	646.803	32.107	32.107	-8.270
78	333.059	652.057	31.280	31.280	-8.270
79	341.642	657.187	30.453	30.453	-8.270
80	350.298	662.192	29.626	29.626	-8.270
81	359.025	667.072	28.799	28.799	-8.270
82	367.822	671.825	27.972	27.972	-8.270
83	376.687	676.451	27.145	27.145	-8.270
84	385.617	680.949	26.318	26.318	-8.270
85	394.611	685.317	25.491	25.491	-8.270
86	403.668	689.555	24.664	24.664	-8.270
87	412.785	693.662	23.837	23.837	-8.270
88	421.960	697.636	23.010	23.009	-8.270
89	431.191	701.478	22.183	22.182	-8.270
90	440.477	705.187	21.356	21.355	-8.270
91	449.816	708.760	20.529	20.528	-8.270
92	459.205	712.199	19.702	19.701	-8.270
93	468.643	715.501	18.875	18.874	-8.270
94	478.127	718.667	18.048	18.047	-8.270
95	487.656	721.697	17.221	17.220	-8.270
96	497.228	724.587	16.394	16.393	-8.270
97	506.840	727.340	15.566	15.566	-8.270
98	516.492	729.954	14.739	14.739	-8.270
99	526.180	732.428	13.912	13.912	-8.270

FIGURE 50. INPUT PARAMETER LISTING FOR "TYPICAL"
 HVOSM CURVE RUN (Continued)

The actual HVOSM simulation runs were performed in batch by use of the interactive remote job entry (RJE) commands.

HVOSM Modifications

A number of refinements and revisions to the HVOSM program were required, including additional outputs of vehicle responses, revision of the path-following driver model, and development of a preprocessing program to simplify the interface between highway definition and HVOSM card inputs. These revisions are described below.

Additional Outputs

Additional calculations and outputs of the existing HVOSM RD2 program were found to be required to enable the evaluation of the curve study. The revisions were as follows:

"Discomfort Factor".--The lateral acceleration output of HVOSM corresponds to measurements made with a "hard-mounted," or body-fixed accelerometer oriented laterally on the vehicle. During cornering, the lateral acceleration of the vehicle is directed toward the center of the turn. On a superelevated turn, the component of gravity that acts laterally on the vehicle is also directed toward the turn center. Thus, the lateral acceleration output is increased by superelevation.

Since the vehicle occupants respond to centrifugal force, their inertial reaction is toward the outside of the turn and therefore the component of gravity that acts laterally on them in a superelevated turn reduces the magnitude of the disturbance produced by cornering. A corresponding program output has been defined to evaluate occupant discomfort in turns.

The effects of a vehicle's roll angle and lateral acceleration on occupants are combined in a "discomfort factor" relationship which represents the net lateral disturbance felt by the occupants (i.e., the occupants' reaction to the combined effects of the lateral acceleration and roll angle).

The "discomfort factor" is coded in the following form:

$$\text{DISCOMFORT FACTOR} = - \text{YLAT} + 1.0 * \text{SIN } \Theta$$

Where: DISCOMFORT FACTOR is in G-units

YLAT = Vehicle Lateral Acceleration in vehicle-fixed coordinate system, G units

Θ = Vehicle roll angle, radians.

Calculations related to the discomfort factor and corresponding outputs were incorporated into the HVOSM.

Friction Demand.--The friction demand is defined to be the ratio of the side force to the normal load of an individual tire. It is indicative of the friction being utilized by each individual tire. The standard outputs of HVOSM include the side force and normal force for each tire. Coding changes were incorporated to calculate and print out the friction demand for each tire at each interval of time.

Driver Model

A recognized problem in the use of either simulation models or full-scale testing in relation to investigations of automobile dynamics is the manner of guiding and controlling the vehicle. Repeatability is essential, and the control inputs must be either representative of an average driver or optimized to achieve a selected maneuver without "hunting" or oscillation. In this investigation of geometric features of highways, the transient portions of the vehicle responses constituted justification for applying a complex computer simulation. The steady-state portions of the vehicle responses can be predicted by means of straightforward hand calculations. Thus, it is essential that the transient responses should not be contaminated by oscillatory steering control inputs.

The Driver model contained in the distributed version of the HVOSM Vehicle Dynamics program was intended to be incorporated into the HVOSM Roadside Design version, but it proved to be inadequate for the present research effort. Therefore, new routines were written for the HVOSM Roadside Design program as described below.

"Wagon-Tongue" Algorithm.--The "wagon-tongue" type of steering control incorporated into the HVOSM Roadside Design Version is one in which the front wheel steer angle is directly proportional to the error of a point on a forward extension of the vehicle X-axis relative to the desired path.

The basic inputs to the "wagon-tongue" algorithm are described in Table 54.

Table 54
INPUTS FOR "WAGON-TONGUE" DRIVER MODEL

<u>Input</u>	<u>Description</u>	<u>Units</u>
TPRB	Time at which driver model is to begin	sec
DPRB	Time between driver model samples	sec
PLGTH	Probe length measured from the center of gravity of the vehicle along the vehicle-fixed X axis	in
PMIN	Null band, minimum acceptable error	in
PMAX	Maximum allowable discomfort factor above which driver model will only reduce steer angle	g-units
PGAIN	Steer correction multiplier--error of probe from desired path multiplied by PGAIN to determine steer correction	rad/in

1 in = 25.4 mm

Desired Path Definition.--The revision to the HVOSM driver model included the incorporation of a "path generating" routine to create a desired path of X,Y data pairs from standard roadway geometric descriptors. Figure 51 lists the path generating routine.

C PATHT.FOR F12
C PATH GENERATOR

30 DECEMBER 1980

J T FLECK

C ROUTINE TO TEST PATH GENERATION SUBROUTINES SETD AND PATHG
C MAY BE USED TO GENERATE DATA SETS FOR TERRAIN GENERATOR
C OR HVOSM

C INPUTS:

C NPTS NUMBER OF POINTS DESIRED
C XINIT X COORDINATE OF FIRST POINT
C YINIT Y COORDINATE OF FIRST POINT
C DELL SPACING BETWEEN POINTS (ALONG STRAIGHT LINE)
C PSA INITIAL HEADING (TANGENT TO PATH)
C KLI NUMBER OF SECTIONS (CURVATURES)
C IF = 0 PROGRAM DEFAULTS TO POINTS IN DATA STATEMENT
C IF > 0 REQUIRES THE FOLLOWING INPUT L = 1, KLI
C DI(L) CURVATURE > 0 RIGHT TURN
C = 0 STRAIGHT
C < 0 LEFT TURN
C RLI(L) DISTANCE FROM INITIAL POINT WHERE DI(L)
C IS EFFECTIVE.
C DISTANCE IS MEASURED IN STRAIGHT LINE
C SEGMENTS BETWEEN POINTS. IF DISTANCE
C 'ALONG ARC IS' REQUIRED SUBROUTINE SETD
C MUST BE MODIFIED.

C NOTE: KLI MAY BE 1 OR GREATER

C E.G. TO GENERATE A STRAIGHT PATH N*DELL UNITS
C LONG AND THEN A RIGHT TURN WITH A CURVATURE OF 20
C INPUT KLI = 1, DI(1) = 20., RLI(1) = N*DELL
C THE ANGLE OF TURN IS GIVEN BY
C $ANGLE = 2 * \arcsin[(DELL/2) * (PI/180) * (DI(L)/100)]$

C OUTPUT

C X(I), Y(I) COORDINATES OF POINT I I = 1 TO NPTS
C DX(I), DY(I) TANGENT AT POINT I (DIRECTION OF PATH)
C D(I) CURVATURE DEFINING PATH FROM POINT I TO POINT I+1

C THESE ARE WRITTEN ON A DATA SET (SY1:PTH.DAT) FOR USE BY OTHER
C ROUTINES

C INTEGER PLOT

C DIMENSION X(100), Y(100), DX(100), DY(100), D(100), DI(100), RLI(100)
C DIMENSION PLOT(70,70)
C DATA RAD/0.01745329/, D /10*0.0, 9*20.0, 9*-20.0, 9*20.0, 63*0.0/
C DATA KLI/0/, DI/100*0.0/, RLI/100*0.0/

C CALL OPEN(6, 'SY1:PTH.DAT ')

C ENTER INITIAL DATA

1 WRITE(1,5)
5 FORMAT(1X, ' ENTER NPTS,XINIT,YINIT,DELL,PSA '/')
READ(1,6)NPTS,XINIT,YINIT,DELL,PSA
6 FORMAT(I4,4F9.0)
IF(NPTS.LT.2)ENDFILE 6
IF(NPTS.LT.2)STOP NPTS

C ENTER # OF CURVATURES (IF 0 ROUTINE USES D SET BY DATA STATEMENT)
C AND OUTPUT UNIT IOUT =0 DEFAULTS TO SCREEN, IOUT =2 FOR PRINTER

WRITE(1,7)
7 FORMAT(' ENTER KLI,IOUT/')
READ(1,11)KLI,IOUT

FIGURE 51. PATH GENERATING ROUTINE

```

11  FORMAT(2I4)
C
    IF(IOUT.EQ.0)IOUT = 1
CHECK IF DI'S AND RLI' ARE TO BE INPUTTED
    IF(KLI.EQ.0)GO TO 17
    DO 15 I =1,KLI
    WRITE(1,14)
14  FORMAT(' ENTER DI, RLI'/)
15  READ(1,16)DI(I),RLI(I)
16  FORMAT(2F9.0)
C
CALL ROUTINE TO COMPUTE D'S FROM DI'S
    CALL SETD(KLI,DI,RLI,NPTS,DELL,D)
C
C INITIALIZE POINTS
17  X(1) = XINIT
    Y(1) = YINIT
C
C INITIALIZE TANGENT
    DX(1) = COS(PSA *RAD)
    DY(1) = SIN(PSA *RAD)
C
CALL ROUTINE TO SET PATH
    CALL PATHG(NPTS,DELL,X,Y,D,DX,DY)
C
    WRITE(6)NPTS,DELL,PSA ,X,Y,DX,DY,D
    WRITE(IOUT,23)NPTS,KLI,DELL,PSA
23  FORMAT(1X,'NPTS=',I4,',', KLI=',',I4,',',DELL=',',F10.4,',',PSA =',',F10.4/)
    IF(KLI.GT.0)WRITE(IOUT,24)(L,DI(L),RLI(L),L=1,KLI)
24  FORMAT(1X,I4,2F10.4)
    WRITE(IOUT,25)
25  FORMAT(/' POINT #      POSITION',19X,'TANGENT',10X,'CURVATURE')
    WRITE(IOUT,26)(I,X(I),Y(I),DX(I),DY(I),D(I),I=1,NPTS)
26  FORMAT(1X,I4,2F10.2,10X,2F10.5,F10.2)
C
C PRINTER PLOT: SPECIAL ROUTINE TO TEST ABOVE DATA
    M = NPTS
    XX = X(1)
    XM = X(1)
    YX = Y(1)
    YM = Y(1)
    DO 35 I =1,M
    IF(X(I).GT.XX)XX = X(I)
    IF(X(I).LT.XM)XM = X(I)
    IF(Y(I).GT.YX)YX = Y(I)
35  IF(Y(I).LT.YM)YM = Y(I)
    SC = XX-XM
    IF(YX-YM.GT.SC)SC = YX-YM
    SX = 60./SC
    SY = 0.6*SX
    DO 38 I=1,70
    DO 38 J=1,70
38  PLOT(I,J) = ' '
    IMAX = 1
    DO 40 K=1,M
    J = (X(K)-XM)*SX +1.
    I = (Y(K)-YM)*SY +1.
    IF(I.GT.IMAX)IMAX = I
40  PLOT(I,J) = '#'
    IF(IOUT.EQ.2)WRITE(2,41)

```

FIGURE 51. PATH GENERATING ROUTINE (Continued)

```

41  FORMAT(1H1)
C
DO 50 I=1,IMAX
LM = 61
DO 44 J=1,60
IF(PLOT(I,LM).NE.' ')GO TO 45
44  LM = LM-1
45  WRITE(IOUT,47)(PLOT(I,L),L=1,LM)
47  FORMAT(5X,71A1)
50  CONTINUE
GO TO 1
END

```

FIGURE 51. PATH GENERATING ROUTINE (Continued)

```

C SUBROUTINE PATH: PATH.FOR F12          30 DECEMBER 1980 J T FLECK
C PATH GENERATOR HVOSM RD-2
C ROUTINE USED IN HVOSM RD-2 TO GENERATE PATH DATA
C
C INPUTS:
C     NPTS          NUMBER OF POINTS DESIRED
C     XINIT         X COORDINATE OF FIRST POINT
C     YINIT         Y COORDINATE OF FIRST POINT
C     DELL          SPACING BETWEEN POINTS (ALONG STRAIGHT LINE)
C     PSA           INITIAL HEADING (TANGENT TO PATH)
C     KLI           NUMBER OF SECTIONS (CURVATURES)
C                   IF = 0 PROGRAM DEFAULTS TO POINTS IN DATA STATEMENT
C                   IF > 0 REQUIRES THE FOLLOWING INPUT   L = 1, KLI
C                   DI(L) CURVATURE > 0 RIGHT TURN
C                           = 0 STRAIGHT
C                           < 0 LEFT TURN
C                   RLI(L) DISTANCE FROM INITIAL POINT WHERE DI(L)
C                           IS EFFECTIVE.
C                           DISTANCE IS MEASURED IN STRAIGHT LINE
C                           SEGMENTS BETWEEN POINTS. IF DISTANCE
C                           ALONG ARC IS REQUIRED SUBROUTINE SETD
C                           MUST BE MODIFIED.
C
C NOTE: KLI MAY BE 1 OR GREATER
C       E.G. TO GENERATE A STRAIGHT PATH N*DELL UNITS
C       LONG AND THEN A RIGHT TURN WITH A CURVATURE OF 20
C       INPUT KLI = 1, DI(1) = 20., RLI(1) = N*DELL
C       THE ANGLE OF TURN IS GIVEN BY
C       ANGLE = 2*ARCSIN[(DELL/2)*(PI/180)*(DI(L)/100)]
C
C OUTPUT
C     X(I), Y(I)    COORDINATES OF POINT I I = 1 TO NPTS
C     DX(I),DY(I)   TANGENT AT POINT I (DIRECTION OF PATH)
C     D(I)          CURVATURE DEFINING PATH FROM POINT I TO POINT I+1
C
C
C SUBROUTINE PATH
C COMMON/PATHD/IPATH ,KLI ,DI(10),RLI(10),
C 1 NPTS,XINIT,YINIT,PSA,DELL,
C 2 X(100),Y(100),DX(100),DY(100),D(100)
C LIMIT ARRAY SIZES
C IF(KLI.GT.10)KLI = 10
C IF(NPTS.GT.100)NPTS = 100
C CALL SETD(KLI,DI,RLI,NPTS,DELL,D)
C SETD WAS MODIFIED ON 30 DEC 1980 TO PRODUCE SPIRAL
C INITIALIZE FIRST POINT AND TANGENT
C X(1) = XINIT
C Y(1) = YINIT
C DX(1) = COS(PSA)
C DY(1) = SIN(PSA)
C
C CALL PATHG(NPTS,DELL,X,Y,D,DX,DY)
C
C RETURN
C END

```

FIGURE 51. PATH GENERATING ROUTINE (Continued,

```

C PROBE.FOR F12          30 DECEMBER 1980          J T FLECK
C SUBROUTINE PROBE:  CALCULATES DISTANCE OF A POINT FROM CENTERLINE
C
C USED IN HVOSM RD-2 MOD'S
C
C INPUTS
C      XP,YP          GIVEN POINT
C      M              NUMBER OF REFERENCE POINTS (= NPTS)
C      X(I), Y(I)     REFERENCE POINTS OF PATH , I =1,NPTS
C      DX(I),DY(I)    TANGENT VECTOR AT REFERENCE POINT
C      D(I)           DEGREE OF CURVATURE AT BETWEEN POINT I AND I+1
C                     D > 0  RIGHT TURN
C                     D = 0  STRAIGHT LINE
C                     D < 0  LEFT TURN
C
C OUTPUTS
C      I              POINT IDENTIFYING SECTOR OF CLOSEST APPROACH
C      DIST           DISTANCE OF POINT FROM ARC
C                     POSITIVE IF POINT IS TO RIGHT OF ARC
C                     NEGATIVE IF POINT IS TO LEFT OF ARC
C      XX ,YY         POINT ON ARC NEAREST GIVEN POINT
C
C NOTE: ON FIRST ENTRY ROUTINE STARTS WITH I = 1, ON SUBSEQUENT
C ENTRIES THE PREVIOUS VALUE OF I IS USED. THIS LOGIC SHOULD BE
C ADEQUATE FOR THE PROPOSED USE OF THE ROUTINE.
C
C      CALCULATION OF XX AND YY MAY BE DELETED IF THIS POINT IS NOT NEEDED
C
C      SUBROUTINE PROBE(XP,YP,M,X,Y,DX,DY,D,I,DIST,XX,YY) .
C      DIMENSION X(1),Y(1),DX(1),DY(1),D(1)
C      DATA RAD/0.017453292519943296/,ILAST/1/
C INITIALIZE
C      I      = ILAST
C      TEST = DX(I)*(XP-X(I))+DY(I)*(YP-Y(I))
C      TSAV = SIGN(1.0,TEST)
C      GO TO 15
C
C START SEARCH
C
C      7      I = I + 1
C             IF(I.LE.M)GO TO 10
C             IF(TSAV.LT.0.0)GO TO 20
C             I = M
C             GO TO 25
C      10     TEST = DX(I)*(XP-X(I))+DY(I)*(YP-Y(I))
C             IF(TEST*TSAV.LE.0.0)GO TO 25
C      15     IF(TEST)20,25,7
C      20     I = I - 1
C             IF(I.GE.1)GO TO 10
C             IF(TSAV.GT.0.0)GO TO 7
C             I = 1
C
C FINISH SEARCH
C      25     IF((TEST.LT.0.0).AND.(I.GT.1))I=I-1
C             ILAST = I
C FINISH OF DETERMINATION OF I

```

FIGURE 51. PATH GENERATING ROUTINE
(Continued)


```

C
CALCULATE DISTANCE
    ZDN = -DY(I)*(XP-X(I))+DX(I)*(YP-Y(I))
    CONS = D(I)*RAD*0.005
    ZDZ = ((XP-X(I))**2+(YP-Y(I))**2)*CONS
    DIST = (ZDN-ZDZ)/(0.5+SQRT(0.25-CONS*(ZDN-ZDZ)))
C
CALCULATE POSITION OF CLOSEST APPROACH POINT ON ARC
C THE FOLLOWING CODE MAY BE DELETED AND THE REFERENCES TO XX AND YY TAKEN
C OUT OF THE CALL IF THE POINT OF CLOSEST APPROACH ON THE ARC IS NOT NEEDED
C
    DEN = 1.0-2.0*DIST*CONS
C
    IF(DEN.GT.0.0)GO TO 30
    WRITE(1,26)I,XP,YP,DIST,DEN
26  FORMAT(' SUBROUTINE PROBE HAS NEGATIVE OR ZERO DENOMINATOR'/
1   ' IN POSITION FORMULA; IMPLIES POINT NOT IN SECTOR'/I6,4F10.4)
    STOP PROBE
C THIS STOP SHOULD NEVER OCCUR IN NORMAL USAGE
C
30  XX = (XP-X(I)+DIST*DY(I))/DEN + X(I)
    YY = (YP-Y(I)-DIST*DX(I))/DEN + Y(I)
35  RETURN
    END
C
C
C*****
C    IF TANGENT VECTOR IS NOT AVAILABLE IT MAY BE REPLACED BY
C        DX = X(I+1)-X(I) , DY = Y(I+1)-Y(I) , I < M
C        DX = X(M) -X(M-1), DY = Y(M) -Y(M-1), I = M
C
C        USE DX FOR DX(I) AND DY FOR DY(I) IN CALCULATION OF TEST
C
C    RETURN CAN BE PUT AT END OF DETERMINATION OF I AND THE
C    DISTANCE AND CALCULATION OF XX,YY DONE BY ANOTHER ROUTINE.
C    (FORMULAS FOR DIST, XX AND YY ARE ONLY VALID FOR CIRCULAR ARCS
C    OR STRAIGHT LINES)

```

FIGURE 51. PATH GENERATING ROUTINE
(Continued)

```

C PATHG.FOR F12          30 DECEMBER 1980          J T FLECK
C  PATH GENERATOR, SUBROUTINE PATHG  HVOSH RD-2
C  INPUTS
C      NPTS          NUMBER OF DESIRED POINTS ( > 1)
C      DELL          SPACING BETWEEN POINTS
C      X(1), Y(1)    INITIAL POSITION SET BY CALLING ROUTINE
C      DX(1),DY(1)   INITIAL TANGENT SET BY CALLING ROUTINE
C      D(I)          DEGREE OF CURVATURE, I = 1 TO NPTS
C                   D(I) > 0  TURN TO RIGHT
C                   D(I) = 0  STRAIGHT
C                   D(I) < 0  TURN TO LEFT
C      NOTE: RADIUS OF CURVATURE IS DEFINED AS
C            EQUAL TO (180/PI)*(100/D) = (5729.6/D)
C            (D HAS DIMENSION OF DEGREES PER 100 UNITS OF DELL)
C
C  OUTPUTS          I = 1 TO NPTS
C      X(I), Y(I)    COORDINATES OF POINTS
C      DX(I),DY(I)   TANGENT VECTOR (DIRECTION OF PATH AT X,Y)
C
C  NOTE: ROUTINE PRODUCES SMOOTH CURVE SUCH THAT TANGENTS ARE CONTINUOUS
C
C      SUBROUTINE PATHG(NPTS,DELL,X,Y,D,DX,DY)
C      DIMENSION X(1),Y(1),DX(1),DY(1),D(1)
C      DATA RAD/0.017453292519943296/
C  INITIALIZE
C      CONS = DELL*RAD/200.0
C*
C      DXX = DELL*DX(1)
C      DYY = DELL*DY(1)
C*
C      DS1 = 0.0
C      DC1 = 1.0
C  START LOOP
C      DO 20 I = 2, NPTS
C      COMPUTE SINE AND COSINE OF HALF SECTOR ANGLE
C      DS2 = CONS*D(I-1)
C      DC2 = SQRT((1.0-DS2)*(1.0+DS2))
C**
C      COMPUTE SINE AND COSINE OF SECTOR ANGLE
C      SP = 2.0*DS2*DC2
C      CP = 1.0 - 2.0*DS2**2
C  UPDATE TANGENT VECTOR
C      DX(I) = CP*DX(I-1) - SP*DY(I-1)
C      DY(I) = SP*DX(I-1) + CP*DY(I-1)
C**
C      COMPUTE SINE AND COSINE OF AVERAGE SECTOR ANGLE
C      SP = DS1*DC2 + DC1*DS2
C      CP = DC1*DC2 - DS1*DS2
C  COMPUTE NEW INCREMENTS
C      DXS = DXX
C      DXX = DXS*CP - DYY*SP
C      DYY = DXS*SP + DYY*CP
C  UPDATE POSITION
C      X(I) = X(I-1) + DXX
C      Y(I) = Y(I-1) + DYY
C  SAVE SINE AND COSINE OF HALF SECTOR ANGLE FOR NEXT I
C      DS1 = DS2
C      DC1 = DC2
C      RETURN
C      END

```

Neuro-Muscular Filter.--The "neuro-muscular" filter from the HVOSM-Vehicle Dynamics Version (Ref. (47), Vol. 3, p. 166-168) was incorporated into the HVOSM Roadside Design version. The filter structure corresponds to the first-order effects of the neurological and muscular systems of a human driver. For the curve study, the following inputs were used for the filter for all runs:

TIL	Time lag of filter	0.05	seconds
TI	Time lead of filter	0.00905	seconds
TAUF	Time delay of filter	0.0	seconds

The related revisions to the Driver model were incorporated into the FHWA distributed Roadside Design version of the HVOSM. However, the revised path-following algorithm was found to produce sustained oscillations about a specified path under some operating conditions. Since the extent of oscillation is dependent on the guidance system parameters as well as the vehicle speed and path curvature, it is possible to obtain peak values of transient response predictions that reflect an artifact of the guidance system rather than a real effect of the highway geometrics under investigation. For example, in Reference (49), comparisons are made between peak transient and steady-state response values which are believed to be more reflective of effects of the guidance system than of the simulated roadway geometrics. Therefore, the following additional modifications were added to the Driver model:

(1) Damping

A damping term (QGAIN) was added to limit the extent of steering activity. Initial runs utilizing the damping term exhibited a reduction in the steering activity as expected. The value used in the curve study was $QGAIN \text{ (rad-sec/m)} = PGAIN/10$, where PGAIN is the steering velocity term described below.

(2) Steer Velocity

In addition to the damping term, an adjustable limit on the steering angle velocity (PGAIN) was incorporated in the path-follower algorithm, enabling the user to limit the maximum instantaneous front wheel steer velocity to a selected value. The value used in the curve study was $PGAIN \text{ (rad/sec)} = 1/\text{Probe Length}$.

(3) Steer Initialization

For runs such as those being performed in relation to the cross-slope break study, the starting point must be relatively close to the cross-slope break to achieve an economical use of computer time. Thus, the input of an initial steer angle to approximate steady-state steer was

required. Previously, the path-follower algorithm was initialized to a steer angle of 0.0 degrees, regardless of the input value for the initial steer angle. Corresponding revisions were made to Subroutine DRIVER to enable input of an initial steer angle.

A revised listing of Subroutine DRIVER, including the cited modifications, is presented in Figure 52.

Terrain Table Generator

The version of the HVOSM maintained by FHWA has the capability of accepting a 3-dimensional definition of the highway surface. The manual generation of these inputs to the HVOSM, however, is time consuming, and the nature and number of geometric configurations to be studied required automation of the procedure.

The automation of the procedure to create terrain tables for the HVOSM consisted of providing an interface between standard roadway geometric descriptions and inputs to the HVOSM. A description of the required inputs to the TTG are as follows:

Centerline Descriptors.--The basic input to the TTG for the generation of centerline points is the radius of curvature of the centerline as a function of distance along the curve. Transitions between descriptors are user controlled and may be spiral or constant. The TTG converts the centerline description into X,Y data pairs and calculates second-order polynomial coefficients for each segment between the data pairs.

Superelevation and/or Gradient Descriptors.--The inputs for the superelevation and gradient are rates as a function of distance along the curve. Transitions between rates are user-controlled and may be spiral or constant.

HVOSM Terrain Table Descriptors.--HVOSM accepts up to four constant increment terrain tables with up to 21 x 21 grid points each as input. Inputs for the TTG to create the HVOSM terrain tables include the definition of the location, size and number of grid points for up to four terrain tables to be created by the TTG.

05/10 C SUBROUTINE DRIVER FOR HVOSH RD-2

```

05720 C
05730 SUBROUTINE DRIVER(PSI,DPSI,JJ,IFLAG,A,B,AMTX,CMGPS)
05740 DIMENSION AMTX(3,3),PPD(50),TPD(50)
05750 COMMON/PATHD/IPATH,KLI,DI(10),RLI(10),NPTS,XINIT,YINIT,
05760 1 PSA,DELL,X(100),Y(100),DX(100),DY(100),D(100)
05770 COMMON/WAGON/IWAGN,TPRB,DPRB,PLGTH,PMIN,PMAX,PGAIN,QGAIN,PSIFD
05780 COMMON/FILT/IFILT,TIL,TI,TMT,TAUF
05790 COMMON/INTG/NEQ,T,DT,VAR(50),DER(50)
05800 COMMON/ACC/CHFCG,CHFA1,CHFA2
05810 DATA NPDMAX/50/,NPD/0/,DPSL/0.0/,N/0/
05820 JJ = 0
05830 IF(IWAGN.EQ.0)GO TO 90
05840 JJ = 1
05850 PSIA = PSI
05860 DTP = DPRB
05870 DPS = 0.0
05880 DPSI = 0.0
05890 IF(IFLAG.EQ.0)GO TO 90
05900 IF(TPRB.GT.T + 0.1*DT)GO TO 10
05910 C COMPUTE NEW CHANGE IN STEER ANGLE
05920 TPRB = TPRB + DPRB
05930 XP = VAR(18) + AMTX(1,1)*PLGTH
05940 YP = VAR(19) + AMTX(2,1)*PLGTH
05950 CALL PROBE(XP,YP,NPTS,X,Y,DX,DY,D,IPRB,DIST,XX,YY)
05960 C SELECTED POINT INDEX IPRB AND LOCATION OF CLOSEST POINT ON PATH XX,YY
05970 C ARE NOT CURRENTLY USED
05980 IF(DIST.EQ.0.0)GO TO 8
05990 SGND=DIST/ABS(DIST)
06000 IF(T.NE.TPRB) DDIST = (DIST-DISTA)/DPRB
06010 9 IF(ABS(DIST).GT.PMIN)DPS = -PGAIN*(ABS(DIST)-PMIN)*SGND
06020 1 -QGAIN*DDIST
06030 8 IF(ABS(DIST).LE.PMIN) DPS= -QGAIN*DDIST
06040 IF(IFILT.EQ.0)GO TO 55
06050 IF(NPD.EQ.NPDMAX)GO TO 10
06060 NPD = NPD + 1
06070 PPD(NPD) = DPS - PSIA
06080 TPD(NPD) = T + TAUF
06090 10 IF(IFILT.EQ.0)GO TO 55
06100 C
06110 C FILTER
06120 C
06130 IF(NPD.EQ.NPDMAX) GO TO 10
06140 TPDTMP = TPD(N)
06150 DO 20 NN = 1,NPD
06160 N = NPD + 1 - NN
06170 20 IF(T.GE.TPD(N))GO TO 30
06180 GO TO 90
06190 30 IF(TPDTMP.LT.TPD(N)) DPSL = 0.0
06200 DPSI = PPD(N)*TMT*EXP(-(T - TPD(N))/TIL)/TIL
06210 DPSN = PPD(N) - TIL*DPSI
06220 DTP = 0.0
06230 DPS = DPSN - DPSL
06240 DPSL = DPSN
06250 IF(NPD.EQ.1)GO TO 50
06260 C
06270 C

```

FIGURE 52. SUBROUTINE DRIVER

```

06280 35 L = 1
06290 DO 40 NN = N,NPD
06300 PPD(L) = PPD(NN)
06310 TPD(L) = TPD(NN)
06320 40 L = L + 1
06330 NPD = L - 1
06340 C
06350 50 PSI = PSIA + DPS
06360 GO TO 58
06370 55 PSI = DPS
06380 58 CONTINUE
06390 C CHECK PREVIOUS TIME INTERVAL COMFORT FACTOR (SEE SUBROUTINE OUTPUT)
06400 C IF GREATER THAN PMAX ALLOW ONLY REDUCTION IN STEER ANGLE
06410 IF((PMAX.GT.0.0).AND.(ABS(CMFA1).LT.PMAX))GO TO 60
06420 IF(ABS(PSI).GT.ABS(PSIA)) PSI=PSIA
06430 60 CONTINUE
06440 C CHECK MAX STEER ANGLE
06450 IF((OMGPS.GT.0.0).AND.(ABS(PSI).GT. OMGPS))
06460 1 PSI = SIGN(OMGPS,PSI)
06470 IF(DTP.NE.0.0)DPSI = (PSI-PSIA)/DTP
06480 C+++ 1/16/81 MCI *****
06490 DPSO = DPS*57.2958
06500 PSIAO = PSIA*57.2958
06510 PSIO = PSI*57.2958
06520 DELPSI = PSIO- PSIAO
06530 XPFT = XP/12.0
06540 YPFT = YP/12.0
06550 XXFT = XX/12.0
06560 YYFT = YY/12.0
06570 C IF(FKD.EQ.1.0) GO TO 90
06580 IF(KPAGE.LE.50.AND.T.NE.0.0000) GO TO 110
06590 WRITE(50,100)
06600 100 FORMAT(
06610 A1H1,33X,37HPROBE COORDINATES PATH COORDINATES,5X,3HPSI,6X,
06620 B3HDPS,6X,4HPSIA,2X,7HDPSI ,2X,7HDPSN ,5HIFLAG,2X,4HIPRB/
06630 C3IH TIME DELTA PSIF ERROR ,6X,1HX,9X,1HY,10X,1HX,8X,1HY/
06640 D3IH (SEC) (DEG) (IN) ,4X,4H(FT),6X,4H(FT),7X,
06650 E4H(FT),5X,4H(FT)/)
06660 KPAGE = 0
06670 110 WRITE(50,120) T,DELPSI,DIST,XPFT,YPFT,XXFT,YYFT,PSIO,DPSO,
06680 A PSIAO,DPSI,DPSN,IFLAG,IPRB
06690 120 FORMAT(1H ,F7.3,2(4X,F7.3),2(3X,F7.1),2X,2(2X,F7.1),3(2X,F7.4),
06700 A 2X,F7.5,2X,F7.5,2X,13,2X,12)
06710 KPAGE = KPAGE + 1
06720 90 RETURN
06730 C*****
06740 END
06750 C*****

```

FIGURE 52. SUBROUTINE DRIVER (Continued)

The TTG calculates the elevation for each terrain table grid point by determining the perpendicular distance from the grid point to the centerline and using that in combination with the superelevation and gradient. The TTG then creates HVOSM card inputs for HVOSM which may be inserted directly into the main HVOSM data deck.

Typical inputs for the TTG are included in Figure 53. The outputs from the TTG consist primarily of either a card or disk data deck for use with HVOSM. Additional diagnostic dumps may also be output to insure the accuracy of the results.

A typical batch job for the TTG costs approximately \$1.00 to \$5.00, dependent on table size, extent of dumps, etc. The cost compares favorably with the hours of manual labor required to create a table manually and indicates that the TTG can provide a useful interface between standard geometric descriptors and HVOSM inputs.

CONTRACT NO. DOT-FH-11-9575, PROGRAMMER-MCHENRY CONSULTANTS, INC., CARY, N.C.

FIGURE 53. TYPICAL TERRAIN TABLE INPUTS FOR HVOSM CURVE STUDY